Oregon State University, Corvallis, OR, U.S.A.), which was followed by incubation with HRP (horseradish peroxidase)-conjugated goat anti-rabbit IgG antibody and HRP-conjugated goat anti-mouse IgG antibody (Santa Cruz Biotechnology, Santa Cruz, CA, U.S.A.) respectively. After washing, the presence of bound HRP was detected by chemiluminescence with an ECL® (enhanced chemiluminescence) Plus detection reagent (Amersham) and exposure to X-ray films. The intensity of each band was quantified by densitometry (ATTO densito graph 4.0, ATTO, Tokyo Japan).

SOD activity assay

RBCs were isolated from venous blood in the presence of EDTA and were washed in ice-cold PBS. Packed cells were washed twice and suspended in 20 mM Tris/HCl, pH 7.4. After centrifugation at 17000 *g* for 15 min, the supernatant was collected and used to assay enzyme activities. SOD activity was determined using WST-1 [2-(4-iodophenyl)-3-(4-nitrophenyl)-5-(2,4-disulphophenyl)-2*H*-tetrazolium] (Wako) for the detection of superoxide anion, as described previously [24]. The reaction mixture contained an appropriate amount of diluted xanthine oxidase (Roche), 0.1 mM xanthine (Wako), 0.025 mM WST-1, 0.1 mM EDTA and 50 mM $NaHCO_3$, pH 10.2, in a total volume of 1 ml. The increase in the absorbance at 438 nm was monitored at 25 °C for 1 min. One unit was defined as the amount of enzyme required to inhibit 50 % of an absorbance change of 0.06/min, multiplied by three. Since this is equivalent to 0.8 units determined by the original standard procedure [25], the presented data corresponded to that of the standard assay after recalculation.

Quantification of antibodies in plasma by ELISA

Anti-CAII (carbonic anhydrase II) antibody was quantified by ELISA as described previously [11]. Assays were performed in duplicate and the absorbance was determined at 495 nm. The anti-HNE (4-hydroxy-2-nonenal) and anti-ACR (acrolein) titers in the plasma samples were measured by ELISA using HNE-modified BSA and ACR-modified BSA respectively, as the coating antigens [26].

Assay for lipid peroxidation

TBARS (thiobarbituric acid-reactive substances) were determined as described previously [11]. TBARS levels were calculated using a molar absorption coefficient of $1.56 \times 10^5\ M^{-1} \cdot cm^{-1}$.

Assay for MetHb (methaemoglobin) content

Fresh RBCs collected from mice were lysed in 50 mM Tris/HCl, pH 6.6. Total haemoglobin and MetHb concentrations in the samples were determined spectrophotometrically. MetHb concentration was determined by comparing the absorbance spectra at 630 nm before and after the addition of potassium cyanide to the haemolysates. MetHb content is expressed as a percentage of total haemoglobin concentration.

Statistical analysis

The Student's *t* test was performed for data from the metabolomic analyses. Statistical analyses of the data were carried out using ANOVA, followed by a post-hoc test when appropriate for other data. $*P < 0.05$, $**;P < 0.01$, $***P < 0.001$.

Table 1 Comparison of the levels of intermediary metabolites in the pentose phosphate pathway in RBCs between *SOD1*$^{+/+}$ and *SOD1*$^{-/-}$ male mice at 7 weeks of age

Metabolomic analyses were performed for RBC samples from two genotypic male mice at 7 weeks of age ($n = 3$ for each group). Intermediary metabolites that are produced in the pentose phosphate pathway, but under detectable levels, are not shown. KO, knockout; WT, wild-type.

Metabolite	*SOD1*$^{+/+}$ (μM)	*SOD1*$^{-/-}$ (μM)	*P* value	Ratio KO/WT
Ribulose 5-phosphate	5.9 ± 0.80	31.4 ± 4.8	0.00082***	5.4
Ribose 5-phosphate	2.1 ± 1.0	12.4 ± 3.1	0.0052**	6.0
Glucose 6-phosphate	82.6 ± 54.7	72.9 ± 40.0	0.82	0.88
Fructose 6-phosphate	36.4 ± 5.5	56.6 ± 21.8	0.20	1.6
6-Phosphogluconate	3.0 ± 0.08	10.5 ± 3.8	0.078	3.4
Sedoheptulose 7-phosphate	7.3 ± 3.7	15.3 ± 9.0	0.22	2.1

RESULTS

Metabolomic analyses of RBCs from *SOD1*$^{-/-}$ mice

We showed that *SOD1*-deficiency causes anaemia, and ultimately, the production of autoantibodies against RBC and renal damage [11]. To gain insight into the metabolic changes in the RBCs that result from elevated ROS, we performed metabolomic analysis of RBCs from *SOD1*$^{-/-}$ male mice and compared the data with *SOD1*$^{+/+}$ littermates at 7 weeks of age. Among the measurable 112 metabolites in RBCs, 37 metabolites showed significant differences (Table 1 and Supplementary Table S1 at http://www.BiochemJ.org/bj/422/bj4220313add.htm) and were classified into three related groups and other compounds: (i) some intermediary metabolites in the pentose phosphate pathway, typically ribulose 5-phosphate and ribose 5-phosphate, which were increased; (ii) various nucleotides, which were also increased in *SOD1*$^{-/-}$ mice; and (iii) among amino acids, 16 increased, but only glutamine was markedly decreased in *SOD1*$^{-/-}$ mice. This result indicates that metabolic flow of carbohydrates shifted from glycolysis to the pentose phosphate pathway (Table 1) and nucleotide synthesis (Supplementary Table S1) without affecting NADPH levels (see Supplementary Figure S1 at http://www.BiochemJ.org/bj/422/bj4220313add.htm).

Generation of *hSOD1*-Tg mice with a *SOD1*$^{-/-}$ background

To understand the role of oxidative stress in RBCs on the phenotype of the *SOD1*$^{-/-}$ mice, we first generated three lines of transgenic mice, designated as TgA, TgB and TgC, that carried and expressed *hSOD1* cDNA under the GATA-1 promoter. *SOD1*-knockout mice were intercrossed with the *hSOD1*$^{tg/+}$ mice, which vary in their levels of hCu,ZnSOD expression in RBCs. In addition to PCR-mediated genotyping of the mice, using specific primers for each genotype, the presence of hCu,ZnSOD in RBCs was confirmed by immunoblot analysis and measurement of SOD activity. Anti-hCu,ZnSOD antibody was used for the immunoblot analysis of proteins in RBCs, so band intensity corresponding to the mouse Cu,ZnSOD was apparently weak (Figure 1A). However, judging from the SOD activity, TgA mice possessed levels of hCu,ZnSOD similar to those of endogenous mouse Cu,ZnSOD (Figure 1C). The erythroid-specific expression of *hSOD1* in the transgenic mice was experimentally verified (Figure 1B). Transgenic expression of hCu,ZnSOD suppressed intracellular ROS levels in RBCs of *SOD1*-knockout mice, although excessive SOD activity in RBCs of *hSOD1*-Tg mice did not have additional ROS scavenging ability measurable

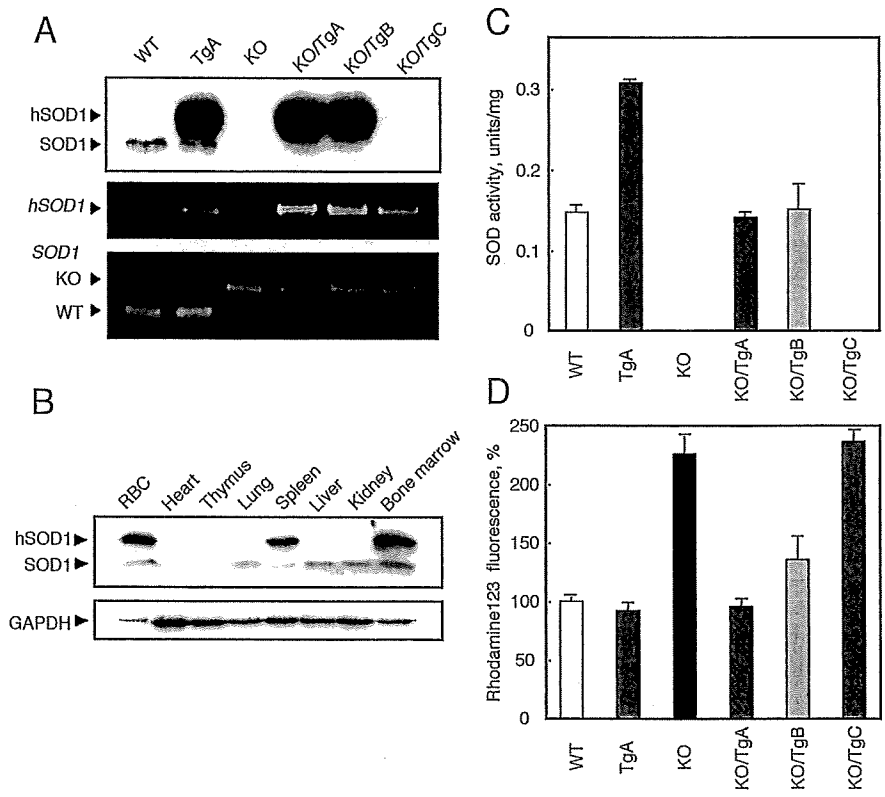

Figure 1 Characterization of *SOD1*-deficient mice carrying the *hSOD1* transgene

(**A**) Immunoblot analyses of the RBC samples from the indicated genetic group of mice were performed using anti-hCu,ZnSOD antibody as a primary antibody. PCR was performed using primers specific for human *SOD1*, or for detecting wild-type (WT) or knockout (KO)*SOD1* alleles. (**B**) Immunoblot analyses were performed for proteins extracted from the indicated tissues of TgA transgenic mice using polyclonal anti-human Cu,ZnSOD antibody. GAPDH (glyceraldehyde-3-phosphate dehydrogenase) was immunoblotted as a loading control. (**C**) Activities of SOD in erythrocytes were measured ($n = 3$, at 10 weeks). (**D**) Blood collected from mice with the indicated genotype was incubated with 25 μM DHR for 15 min, followed by FACS analysis. The relative fluorescence intensity of RBCs from these mice is shown ($n = 5$, at 10 weeks).

by DHR (Figure 1D). In the following experiments, using three lines of hSOD1$^{tg/+}$ mice, we focused our analysis on the TgA and TgA-derived mouse lines that possessed an amount of hCu,ZnSOD activity equivalent to the endogenous mouse Cu,ZnSOD activity.

Effects of the *hSOD1* transgene on the anaemic phenotype of mice

We generated F1 mice by intercrossing *SOD1*$^{+/-}$; *hSOD1*$^{tgA/+}$ and maintained four genetic groups of mice, *SOD1*$^{+/+}$, TgA (*SOD1*$^{+/+}$;*hSOD1*$^{tgA/+}$), *SOD1*$^{-/-}$ and KO/TgA (*SOD1*$^{-/-}$;*hSOD1*$^{tgA/+}$). With respect to the viability of RBCs, transgenic expression of *hSOD1* in KO/TgA mice fully extended the shortened lifespan of RBCs that was observed in the *SOD1*$^{-/-}$ mice, and made it comparable with those of *SOD1*$^{+/+}$ mice (Figure 2A). No further prolongation of lifespan was observed in TgA mice, consistent with intracellular ROS levels that were the same as *SOD1*$^{+/+}$. The anaemic phenotype observed in *SOD1*$^{-/-}$ mice was significantly improved by transgenic expression of *hSOD1* in the RBCs of KO/TgA mice, particularly at young ages (Figure 2B). Splenomegaly, an indication of excess destruction of RBCs in *SOD1*$^{-/-}$ mice, was also significantly suppressed by the transgenic expression of *hSOD1* (Figure 2C). These data suggest that Cu,ZnSOD deficiency in RBCs accelerated destruction and caused anaemia in *SOD1*$^{-/-}$ mice, and that the complement of SOD activity by transgenic expression of *hSOD1* only in erythroid cells could effectively rescue the phenotypes, especially at young ages.

Suppression of oxidative stress by expression of the transgene in RBCs

To elucidate the causal connection between anaemia and the oxidation state of RBCs, we examined ROS, MetHb contents, and lipid peroxidation products in the RBCs of the four genetic groups of mice. ROS levels in RBCs, as assessed by DHR fluorescence, were extremely high in *SOD1*$^{-/-}$ mice, but the levels in KO/TgA mice were approximately the same as those in *SOD1*$^{+/+}$ and TgA mice by 30 weeks, although they gradually increased subsequently (Figure 3A). MetHb content, an indicator of haemoglobin oxidation in RBCs, was also elevated in *SOD1*$^{-/-}$ mice, but was normal in KO/TgA mice (Figure 3B). We also measured lipid peroxidation products in the four genetic groups, as determined by measurement of TBARS, and found approximately normal levels of lipid peroxidation products in the KO/TgA group, compared with those of the *SOD1*$^{-/-}$ and *SOD1*$^{+/+}$ groups (Figures 3C). Thus, the significant oxidative stress observed in *SOD1*$^{-/-}$ mice was effectively suppressed simply by production of hCuZnSOD in RBCs, although the suppressive effect of the transgene on the oxidative stress appeared to weaken during aging.

Among various injurious ROS, we hypothesized that peroxynitrite is a putative impairing species and attempted to provide evidence by determining 3-nitrotyrosine, a marker for protein modification by peroxynitrite, in RBC proteins by immunoblot analyses using anti-3-nitrotyrosine antibodies. As a result, however, we found no reactive bands in RBC proteins from *SOD1*$^{-/-}$ and *SOD1*$^{+/+}$ mice (results not shown). When RBCs were incubated with 100 μM SIN-1 (3-morpholinosydnonimine),

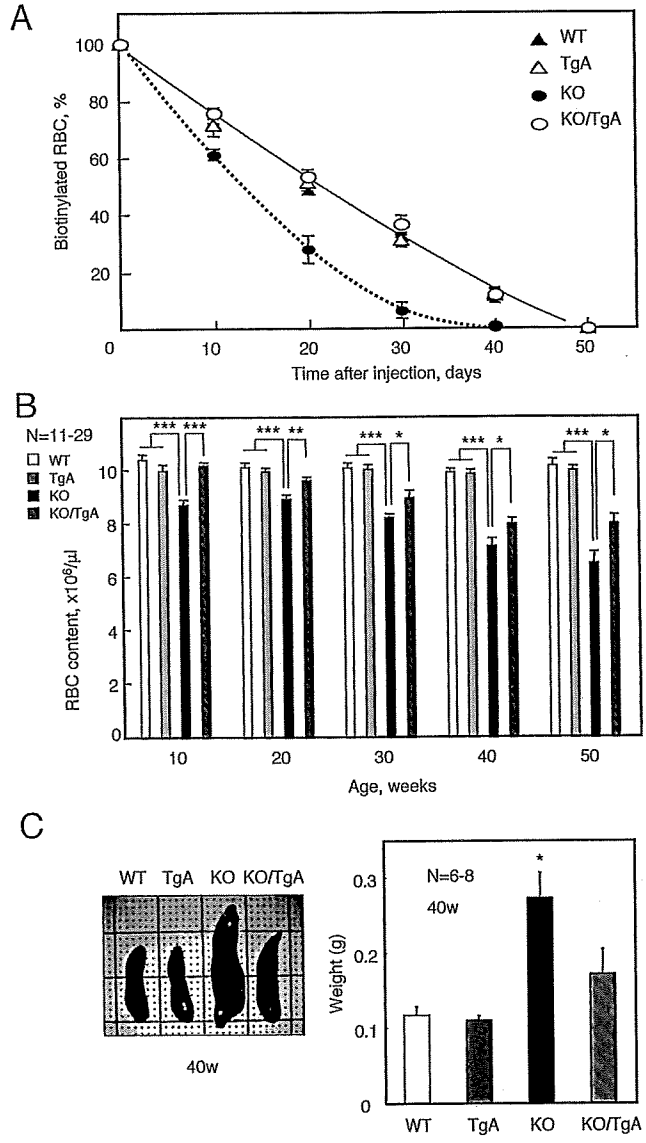

Figure 2 Effects of the *hSOD1* transgene on anaemic phenotypes of *SOD1*-deficient mice

(**A**) NHS-LC-biotin [succinimidyl-6-(biotinamido)hexanoate] was intravenously injected into 15-week-old mice at day 0. At the indicated time points, an aliquot of blood was reacted with phycoerythrin-conjugated streptavidin, followed by FACS analysis to determine the fraction of labelled RBCs remaining in the blood at the indicated time point ($n = 3$). (**B**) RBC content in the blood of the mice was measured at 10, 20, 30, 40 and 50 weeks after birth ($n = 11$–29). (**C**) Spleens were dissected from mice and weighed at 40 weeks of age ($n = 5$–8). KO, knockout; WT, wild-type.

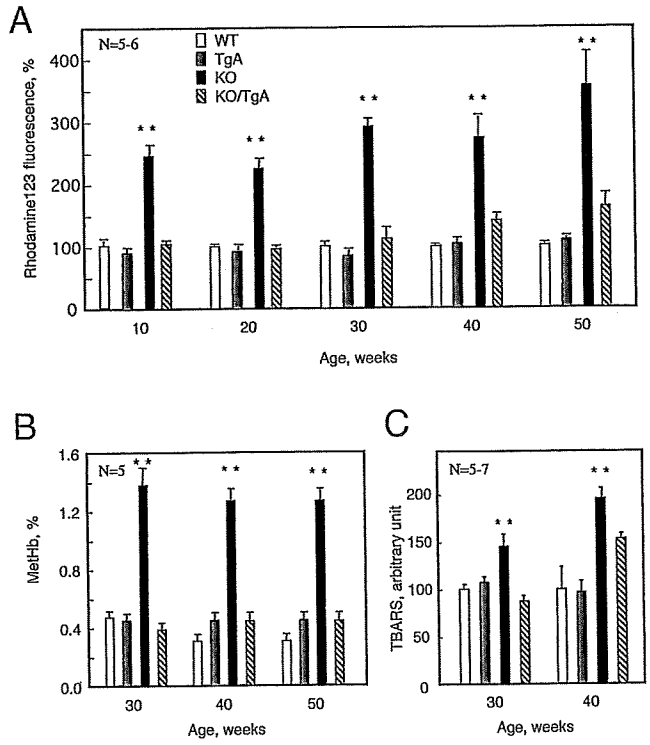

Figure 3 Oxidation state of RBCs in four genetic groups of mice

(**A**) Blood collected from mice with the indicated genotype was incubated with 25 μM DHR for 15 min, followed by FACS analysis as described in Figure 1(C). The relative fluorescence intensity of RBCs from these mice is shown at the indicated ages. (**B**) MetHb contents in RBCs were measured in mice at 30, 40 and 50 weeks of age ($n = 5$). (**C**) Lipid peroxidation products in the membranes of RBCs from the mice at 30 and 40 weeks were quantified as TBARS ($n = 5$–7). KO, knockout; WT, wild-type.

which produces NO and superoxide simultaneously and is regarded as a peroxynitrite donor, elevation of peroxides judged by APF fluorescence (Figure 4A), TBARS (Figure 4B) and MetHb contents (Figure 4C) were observed notably in the RBCs of *SOD1*$^{-/-}$ mice. However, again, there was no increase in the level of 3-nitrotyrosine in proteins of RBCs treated with ~1 mM SIN-1 for 1 h, although nitrated bovine serum albumin reacted with the antibody (results not shown).

Suppression of autoantibody production and improved kidney function by transgenic expression of *hSOD1*

Since the production of autoantibodies against RBCs occurs in *SOD1*$^{-/-}$ mice [11], we measured and compared the levels of certain antibodies in plasma among the four genetic groups of mice. Although an increase in the level of IgG bound to RBCs was confirmed in the *SOD1*$^{-/-}$ group mice, the level in the KO/TgA group was as low as that observed in the *SOD1*$^{+/+}$ and TgA groups until 40 weeks, but increased in aged mice, as observed in the *SOD1*$^{-/-}$ group (Figure 5A). Since antibodies against lipid peroxidation products such as HNE are found in some autoimmune diseases [26,27], we measured the levels of antibodies in mouse blood plasma that bound HNE- and acrolein-modified BSA. Antibodies against these were elevated only in *SOD1*$^{-/-}$ mouse plasma, but were nearly the same in the *SOD1*$^{+/+}$ and TgA groups at 50 weeks (Figures 5B and 5C). Levels of the anti-CAII antibody, which are elevated in SLE and Sjögren's syndrome [28], showed approximately the same profile as the antibodies against the lipid peroxidation products (Figure 5D). We also examined kidney function by measurement of BUN in the four groups of mice at 50 weeks. BUN was significantly elevated in *SOD1*$^{-/-}$ mice, but was nearly normal in the KO/TgA group of mice (Figure 5E), suggesting that the impaired kidney function in the *SOD1*$^{-/-}$ mice was improved by transgenic production of hCu,ZnSOD in RBCs. Because the production of hCu,ZnSOD in RBCs alone could rescue most phenotypes in mice with a *SOD1*$^{-/-}$ background, RBC oxidative stress appears to be a cause of anaemia and autoantibody production.

DISCUSSION

Recently, we reported that the elevation of ROS and consequent oxidation of proteins and lipids occur in RBCs and lead to anaemia

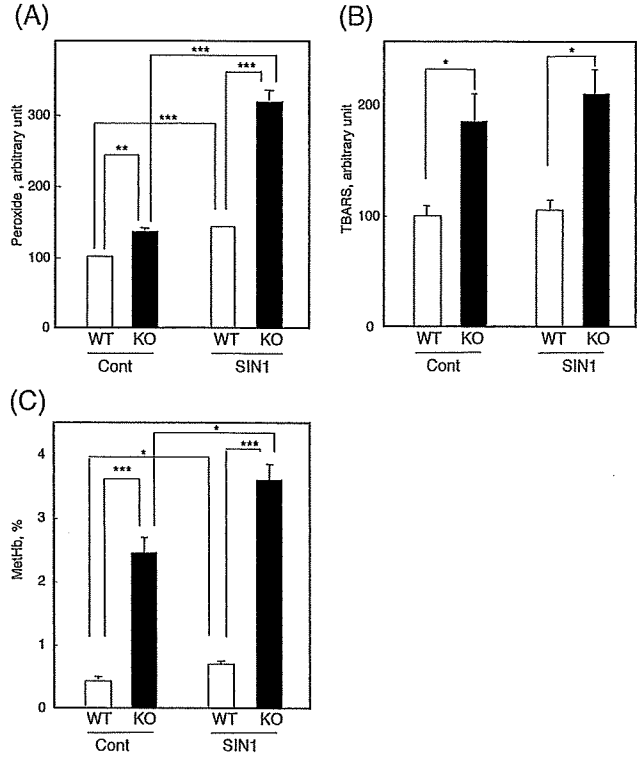

Figure 4 Effects of peroxynitrite-generating donor SIN-1 on RBCs from *SOD1*$^{-/-}$ and *SOD1*$^{+/+}$ mice

(**A**) RBCs isolated from male *SOD1*$^{-/-}$ (KO) and *SOD1*$^{+/+}$ (WT) mice at 10–14 weeks ($n=3$) were incubated with 0, 100 and 500 μM SIN-1 for 30 min at 37 °C. Immunoblot analysis using anti-3-nitrotyrosine antibody was performed. (**B** and **C**) RBCs were preincubated with 10 μM APF for 10 min and then incubated with 100 μM SIN-1. Fluorescence intensity of RBCs was detected by FACS at 515 nm. After treatment with 100 μM SIN-1, levels of TBARS (**B**) and MetHb (**C**) were measured. KO, knockout; WT, wild-type.

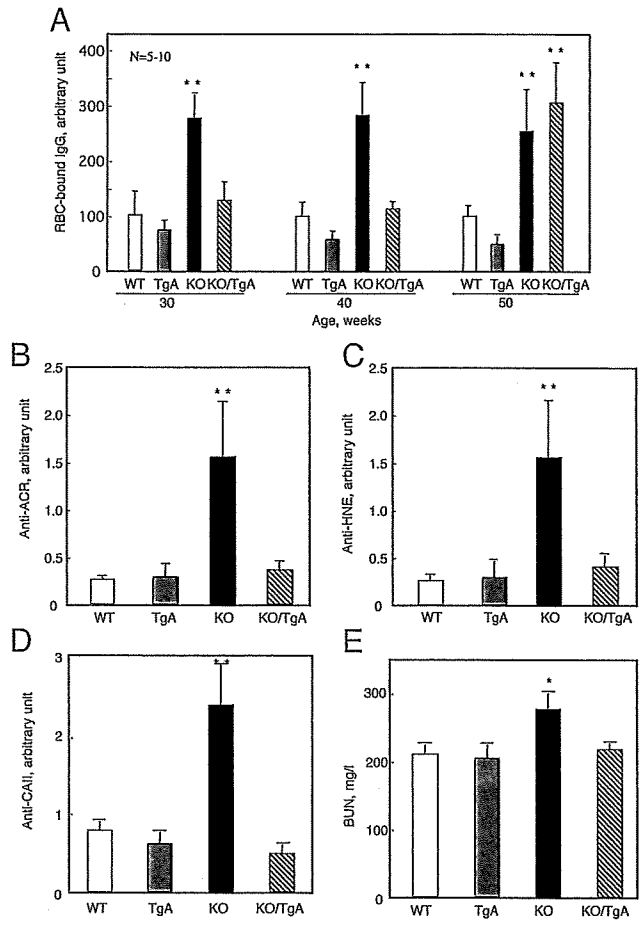

Figure 5 Suppression of IgG bound to RBCs and production of antibodies by the *hSOD1* transgene

(**A**) RBCs collected from mice at 30, 40 and 50 weeks were incubated with FITC-labelled anti-mouse IgG, followed by FACS analysis. The relative values of bound IgG are shown ($n=5$–6). Quantification of antibodies against acrolein (**B**) and HNE (**C**) in blood plasma from 50-week-old mice is shown. (**D**) Relative values of anti-CAII antibody in plasma from 50-week-old mice are shown ($n=5$–6). (**E**) Levels of BUN from 50-week-old mice are shown. KO, knockout; WT, wild-type.

[11]. Based on these observations, we hypothesized that ROS production plays a causative role in anaemia and the autoimmune response against RBCs. In the present paper we present evidence that supports the causal connection between oxidative stress and autoantibody production by generating and characterizing a *SOD1*$^{-/-}$;*hSOD1*$^{tg/+}$ mouse that expressed *hSOD1* in an erythroid cell-specific manner. The possible participation of a defective immune system in autoantibody production in *SOD1*-deficient mice was thus clearly eliminated. Since the *hSOD1* transgene improved anaemia, oxidative modification of RBCs and production of autoantibodies, all these phenotypes could be attributed to the inability to detoxify superoxide in Cu,ZnSOD-deficient RBCs.

SOD catalyses the dismutation of superoxide to hydrogen peroxide and oxygen, so that Cu,ZnSOD deficiency only slows down the formation of hydrogen peroxide from superoxide. However, formation of peroxynitrite would be enhanced because superoxide remains high in the RBCs of *SOD1*$^{-/-}$ mice. When we examined the levels of 3-nitrotyrosine in RBC proteins, no difference was observed between *SOD1*$^{-/-}$and *SOD1*$^{+/+}$ mice (Figure 4). Incubation of RBCs with a peroxynitrite donor SIN-1 ($\sim$500 μM) elevated oxidative stress, but did not increase the level of 3-nitrotyrosine. These results can be explained by a catalytic function of oxyhaemoglobin that is present at 5 mM and efficiently isomerizes peroxynitrite to nitrate [29]. Although 3-nitrotyrosine formation is reported in RBC proteins [30], extremely high levels of peroxynitrite was used. Romero et al. [29] have shown that physiological levels of peroxynitrite are rapidly converted into nitrate by oxyhaemoglobin without significant formation of 3-nitrotyrosine. These mechanisms would explain why we did not detect 3-nitrotyroinse in the RBCs of *SOD1*$^{-/-}$ mice. On the other hand, plasma membrane lipids would easily undergo oxidation by peroxynitrite that is produced from superoxide produced intracellularly and by NO that is produced extracellularly prior to isomerization by oxyhaemoglobin. We actually observed elevated lipid peroxidation in the RBCs of the *SOD1*$^{-/-}$ mice and *in vitro* by incubation with peroxynitrite donor SIN-1 without 3-nitrotyrosine formation (Figure 4).

Moreover, we showed that antibodies against lipid peroxidation products, HNE and ACR, were also elevated in *SOD1*-deficient mice (Figure 5). Kidney dysfunction, which is typically seen in lupus nephritis [31], was also evident in *SOD1*-deficient mice. Since the *SOD1*-knockout mice completely lack Cu,ZnSOD, we were careful to acknowledge the possibility that defects in the immune system due to oxidative stress may be involved in autoantibody production. Our approach utilized transgenic expression of *hSOD1* only in RBCs, to determine whether hCu,ZnSOD could rescue the phenotypes with respect to autoimmune responses. In the resulting KO/TgA mice, the transgene product suppressed levels of ROS and oxidation

products in RBCs to an extent similar to $SOD1^{+/+}$ mice (Figure 3). The transgene product normalized the lifespan of RBCs and improved the anaemic phenotype (Figure 2). In a similar fashion, the production of IgG against RBCs, and other antibodies, was suppressed to normal levels (Figure 5). All these data support the hypothetical role of ROS in autoantibody production against RBCs in CuZnSOD-deficient RBCs. Thus, these data clearly eliminate the possible involvement of a defect in the immune system, and suggest that the increase in RBC ROS due to *SOD1* deficiency is responsible for the above phenotypes, including the autoimmune response.

While the most antigenic protein in RBCs is the Band III protein in AIHA [32–34], modification, such as oxidation and proteolysis, can increase the antigenicity of several RBC proteins [35,36]. When an AIHA-prone NZB (New Zealand Black) mouse was back-crossed with a mutant mouse lacking the *AE1* allele, the gene encoding the Band III protein, this resulted in *AE1*-deficient NZB mice with an autoimmune response to RBCs and the production of an autoantibody against glycophorin, another predominant membrane protein of RBCs [37]. This suggests that besides the Band III protein, RBCs also are preferential antigens in AIHA, and lipid peroxidation products in RBCs could be promising candidates. In fact, a significant amount of anti-HNE antibody is present in the plasma of SLE patients [26]. Analysis of oxidative stress parameters in the blood and RBCs of SLE patients showed that plasma concentrations of HNE, as well as malondialdehyde and oxidized glutathione, increased [27]. In this study, the elevation of antibodies against HNE and acrolein occurred concomitantly with the increase in the IgG bound to RBCs in $SOD1^{-/-}$ mice (Figure 5). Thus at least part of the IgG bound to RBCs may be antibodies against lipid peroxidation products, such as HNE. Some oxidation products, which are aldehyde compounds similar to HNE, are still reactive and modify proteins [38], whereas modification with HNE increases the antigenicity of proteins and nucleotides [26,39,40].

We also asked how elevated ROS are involved in RBC destruction and the onset of anaemia. The data from metabolomic analysis of Cu,ZnSOD-deficient RBCs clearly indicated upregulation of glucose metabolism and a shift in carbohydrate metabolism from glycolysis to the pentose phosphate pathway (see Table 1 and Supplementary Table S1), although part of the difference in the content of metabolites is attributable to a shortened life span and to elevated erythropoiesis in SOD1-deficient mice. Prior to this analysis, we speculated that the most common cause for human anaemia is deterioration of the pentose phosphate pathway because of a deficiency in G6PD (glucose-6-phophate dehydrogenase), which catalyses the first rate-determining step of the pentose phosphate pathway [41]. A major component of the haemolytic process in G6PD deficiency can be attributed to the inability of RBCs to protect sulfhydryl groups against ROS [38]. Indeed, an elevation in taurine indicates accelerated oxidation of cysteine metabolism in the RBCs of *SOD1*-deficient mice. Thus, anaemia in $SOD1^{-/-}$mice appears to be based on a mechanism different from G6PD deficiency.

Although mice lacking *GPX1*, which encodes a major glutathione peroxidase in RBCs, show a normal phenotype [42], anaemia is caused by deficiency of peroxiredoxin 2, which is a thioredoxin-dependent peroxidase and is the third most abundant protein in RBCs [43]. This result suggests that glutathione-dependent peroxidation is not a major protective mechanism, but that a thioredoxin/peroxidredoxin 2 system is more important in the protection of RBCs by eliminating ROS. The protective mechanism of peroxiredoxin 2 against hydrogen peroxide appears to be due to a noncatalytic scavenging function via reactive sulfhydryl groups of the protein [44]. RBCs require a continual supply of NADPH for reductase reactions, such as thioredoxin reductase and glutathione reductase, to maintain the redox balance [45]. Although NADH is produced during glycolysis, the reducing equivalent is mainly used to reduce continuously produced MetHb to oxygen-carrying haemoglobin and pyruvate to lactate [14]. Thus, the pentose phosphate pathway would play a pivotal role by providing NADPH for the survival of RBCs under oxidative stress. However, there was no difference in the oxidation state of NADPH between RBCs of $SOD1^{-/-}$ and $SOD1^{+/+}$ mice (see Supplementary Figure S1), which might be attributable to quick recovery by the activated pentose phosphate pathway.

The estimated half-life of ATP in RBCs is 1 h, which is much longer than that in reticulocytes (40 s) in rabbits [46]. This means that, in healthy RBCs, the energy charge potential can be maintained by very low glycolytic activity compared with that in other cells. Thus, in addition to oxidative modification of RBCs, low energy charge potential due to elevated ATP consumption by nucleotide synthesis may also be responsible for reducing the lifespan of RBCs, leading to anaemia in *SOD1*-deficient mice.

In conclusion, we have provided unambiguous evidence for the involvement of oxidative stress in the autoimmune response. Oxidative stress due to *SOD1* deficiency shifts glucose metabolism from glycolysis to the pentose phosphate pathway and results in decreased energy charge potential. Collectively, these changes accelerate destruction of RBCs and lead to anaemia. Antibodies are then produced against the oxidation products and may trigger the autoimmune reaction, as found in AIHA and related autoimmune diseases.

AUTHOR CONTRIBUTION

Yoshihito Iuchi, Futoshi Okada, Rina Takamiya, Noriko Kibe, Satoshi Tsunoda, Osamu Nakajima, Kazuyo Toyoda and Ritsuko Nagae were responsible for performing experiments. Rina Takamiya, Makoto Suematsu and Tomoyoshi Soga contributed to metabolomic analyses. Makoto Suematsu, Tomoyoshi Soga, Koji Uchida and Junichi Fujii were responsible for planning experiments, analysing data and writing the manuscript.

ACKNOWLEDGEMENTS

We thank Professor Masayuki Yamamoto, Tohoku University, for the gift of the vector plasmid IE3.9int.

FUNDING

This work was supported, in part, by the Global COE Program (F03) from the Japan Society for the Promotion of Science (JSPS). The metabolome analysis was supported by the Global COE Program for Life Sciences, titled Human Metabolomic Systems Biology, from MEXT (Ministry of Education, Culture, Sports, Science and Technology).

REFERENCES

1 Sies, H. (1991) In Oxidative Stress II. Oxidants and Antioxidants. Academic Press, London
2 Rhee, S. G., Kang, S. W., Jeong, W., Chang, T. S., Yang, K. S. and Woo, H. A. (2005) Intracellular messenger function of hydrogen peroxide and its regulation by peroxiredoxins. Curr. Opin. Cell Biol. **17**, 183–189
3 Fridovich, I. (1995) Superoxide radical and superoxide dismutases. Annu. Rev. Biochem. **64**, 97–112
4 Okado-Matsumoto, A. and Fridovich, I. (2001) Subcellular distribution of superoxide dismutases (SOD) in rat liver: Cu,Zn-SOD in mitochondria. J. Biol. Chem. **276**, 38388–38393
5 Ho, Y. S., Gargano, M., Cao, J., Bronson, R. T., Heimler, I. and Hutz, R. J. (1998) Reduced fertility in female mice lacking copper-zinc superoxide dismutase. J. Biol. Chem. **273**, 7765–7769
6 Matzuk, M. M., Dionne, L., Guo, Q., Kumar, T. R. and Lebovitz, R. M. (1998) Ovarian function in superoxide dismutase 1 and 2 knockout mice. Endocrinology **139**, 4008–4011

7 Li, Y., Huang, T. T., Carlson, E. J., Melov, S., Ursell, P. C., Olson, J. L., Noble, L. J., Yoshimura, M. P., Berger, C., Chan, P. H. et al. (1995) Dilated cardiomyopathy and neonatal lethality in mutant mice lacking manganese superoxide dismutase. Nat. Genet. **11**, 376–381
8 Reaume, A. G, Elliott, J. L, Hoffman, E. K, Kowall, N. W, Ferrante, R. J, Siwek, D. F, Wilcox, H. M, Flood, D. G, Beal, M. F, Brown, Jr, R. H et al. (1996) Motor neurons in Cu/Zn superoxide dismutase-deficient mice develop normally but exhibit enhanced cell death after axonal injury. Nat. Genet. **3**, 43–47
9 Shefner, J. M, Reaume, A. G, Flood, D. G, Scott, R. W, Kowall, N. W, Ferrante, R. J, Siwek, D. F, Upton-Rice, M and Brown, Jr, R. H (1999) Mice lacking cytosolic copper/zinc superoxide dismutase display a distinctive motor axonopathy. Neurology **53**, 1239–1246
10 Yoshida, T., Maulik, N., Engelman, R. M., Ho, Y. S. and Das, D. K. (2000) Targeted disruption of the mouse Sod I gene makes the hearts vulnerable to ischemic reperfusion injury. Circ. Res. **86**, 264–269
11 Iuchi, Y., Okada, F., Onuma, K., Onoda, T., Asao, H., Kobayashi, M. and Fujii, J. (2007) Elevated oxidative stress in erythrocytes due to an SOD1 deficiency causes anemia and triggers autoantibody production. Biochem. J. **402**, 219–227
12 Grzelak, A., Kruszewski, M., Macierzyńska, E., Piotrowski, Ł., Pułaski, Ł., Rychlik, B. and Bartosz, G. (2009) The effects of superoxide dismutase knockout on the oxidative stress parameters and survival of mouse erythrocytes. Cell. Mol. Biol. Lett. **14**, 23–34
13 Starzyński, R. R., Canonne-Hergaux, F., Willemetz, A., Gralak, M. A., Woliński, J., Styś, A., Olszak, J. and Lipiński, P. (2009) Hemolytic anemia and alterations in hepatic iron metabolism in aged mice lacking Cu,Zn-superoxide dismutase. Biochem. J. **420**, 383–390
14 Winterbourn, C. C. (1990) Oxidative reactions of hemoglobin. Methods Enzymol. **186**, 265–272
15 Radi, R (2004) Nitric oxide, oxidants, and protein tyrosine nitration. Proc. Natl. Acad. Sci. U.S.A. **101**, 4003–4008
16 Arese, P., Turrini, F. and Schwarzer, E. (2005) Band 3/complement-mediated recognition and removal of normally senescent and pathological human erythrocytes. Cell Physiol. Biochem. **16**, 133–146
17 Izui, S. (1994) Autoimmune hemolytic anemia. Curr. Opin. Immunol. **6**, 926–930
18 Kurien, B. T., Hensley, K., Bachmann, M. and Scofield, R. H. (2006) Oxidatively modified autoantigens in autoimmune diseases. Free Radical Biol. Med. **41**, 549–556
19 Sokol, R. J. and Hewitt, S. (1985) Autoimmune hemolysis: a critical review. Crit. Rev. Oncol. Hematol. **4**, 125–154
20 Suganuma, K., Tsukada, K., Kashiba, M., Tsuneshige, A., Furukawa, T., Kubota, T., Goda, N., Kitajima, M., Yonetani, T. and Suematsu, M. (2006) Erythrocytes with T-state-stabilized hemoglobin as a therapeutic tool for postischemic liver dysfunction. Antioxid. Redox Signal. **8**, 1847–1855
21 Kinoshita, A., Tsukada, K., Soga, T., Hishiki, T., Ueno, Y., Nakayama, Y., Tomita, M. and Suematsu, M. (2007) Roles of hemoglobin allostery in hypoxia-induced metabolic alterations in erythrocytes: simulation and its verification by metabolome analysis. J. Biol. Chem. **282**, 10731–10741
22 Soga, T., Baran, R., Suematsu, M., Ueno, Y., Ikeda, S., Sakurakawa, T., Kakazu, Y., Ishikawa, T., Robert, M., Nishioka, T. and Tomita, M. (2006) Differential metabolomics reveals ophthalmic acid as an oxidative stress biomarker indicating hepatic glutathione consumption. J. Biol. Chem. **281**, 16768–16776
23 Onodera, K., Takahashi, S., Nishimura, S., Ohta, J., Motohashi, H., Yomogida, K., Hayashi, N., Engel, J. D. and Yamamoto, M. (1997) GATA-1 transcription is controlled by distinct regulatory mechanisms during primitive and definitive erythropoiesis. Proc. Natl. Acad. Sci. U.S.A. **94**, 4487–4492
24 Otsu, K., Ikeda, Y. and Fujii, J. (2004) Accumulation of manganese superoxide dismutase under metal-depleted conditions: proposed role for zinc ions in cellular redox balance. Biochem. J. **377**, 241–248
25 McCord, J. M. and Fridovich, I. (1969) Superoxide dismutase. An enzymic function for erythrocuprein (hemocuprein). J. Biol. Chem. **244**, 6049–605
26 Toyoda, K., Nagae, R., Akagawa, M., Ishino, K., Shibata, T., Ito, S., Shibata, N., Yamamoto, T., Kobayashi, M., Takasaki, Y. et al. (2007) Protein-bound 4-hydroxy-2-nonenal: an endogenous triggering antigen of anti-DNA response. J. Biol. Chem. **282**, 25769–25778
27 Gil, L., Siems, W., Mazurek, B., Gross, J., Schroeder, P., Voss, P. and Grune, T. (2006) Age-associated analysis of oxidative stress parameters in human plasma and erythrocytes. Free Radical Res. **40**, 495–505
28 Inagaki, Y., Jinno-Yoshida, Y., Hamasaki, Y. and Ueki, H. (1991) A novel autoantibody reactive with carbonic anhydrase in sera from patients with systemic lupus erythematosus and Sjögren's syndrome. J. Dermatol. Sci. **2**, 147–154
29 Romero, N., Radi, R., Linares, E., Augusto, O., Detweiler, C. D., Mason, R. P. and Denicola, A. (2003) Reaction of human hemoglobin with peroxynitrite. Isomerization to nitrate and secondary formation of protein radicals. J. Biol. Chem. **278**, 44049–44057
30 Pietraforte, D., Matarrese, P., Straface, E., Gambardella, L., Metere, A., Scorza, G., Leto, T. L., Malorni, W. and Minetti, M. (2007) Two different pathways are involved in peroxynitrite-induced senescence and apoptosis of human erythrocytes. Free Radical Biol. Med. **42**, 202–214
31 Suwannaroj, S., Lagoo, A., Keisler, D. and McMurray, R. W. (2001) Antioxidants suppress mortality in the female NZB × NZW F1 mouse model of systemic lupus erythematosus (SLE). Lupus **10**, 258–265
32 Barker, R. N., de Sa Oliveira, G. G., Elson, C. J. and Lydyard, P. M. (1993) Pathogenic autoantibodies in the NZB mouse are specific for erythrocyte band 3 protein. Eur. J. Immunol. **23**, 1723–1726
33 Poole, J. (2000) Red cell antigens on band 3 and glycophorin A. Blood Rev. **14**, 31–43
34 Shen, C. R., Youssef, A. R., Devine, A., Bowie, L., Hall, A. M., Wraith, D. C., Elson, C. J. and Barker, R. N. (2003) Peptides containing a dominant T-cell epitope from red cell band 3 have *in vivo* immunomodulatory properties in NZB mice with autoimmune hemolytic anemia. Blood **102**, 3800–3806
35 Beppu, M., Mizukami, A., Nagoya, M. and Kikugawa, K. (1990) Binding of anti-band 3 autoantibody to oxidatively damaged erythrocytes. Formation of senescent antigen on erythrocyte surface by an oxidative mechanism. J. Biol. Chem. **265**, 3226–3233
36 Fossati-Jimack, L., Azeredo da Silveira, S., Moll, T., Kina, T., Kuypers, F. A., Oldenborg, P. A., Reininger, L. and Izui, S. (2002) Selective increase of autoimmune epitope expression on aged erythrocytes in mice: implications in anti-erythrocyte autoimmune responses. J. Autoimmun. **18**, 17–25
37 Hall, A. M., Ward, F. J., Shen, C. R., Rowe, C., Bowie, L., Devine, A., Urbaniak, S. J., Elson, C. J and and Barker, R. N. (2007) Deletion of the dominant autoantigen in NZB mice with autoimmune hemolytic anemia: effects on autoantibody and T-helper responses. Blood **110**, 4511–4517
38 Uchida, K. (2003) 4-Hydroxy-2-nonenal: a product and mediator of oxidative stress. Prog. Lipid Res. **42**, 318–343
39 Scofield, R. H., Kurien, B. T., Ganick, S., McClain, M. T., Pye, Q., James, J. A., Schneider, R. I., Broyles, R. H., Bachmann, M. and Hensley, K. (2005) Modification of lupus-associated 60-kDa Ro protein with the lipid oxidation product 4-hydroxy-2-nonenal increases antigenicity and facilitates epitope spreading. Free Radical Biol. Med. **38**, 719–728
40 Akagawa, M., Ito, S., Toyoda, K., Ishii, Y., Tatsuda, E., Shibata, T., Yamaguchi, S., Kawai, Y., Ishino, K., Kishi, Y. et al. (2006) Bispecific Abs against modified protein and DNA with oxidized lipids. Proc. Natl. Acad. Sci. U.S.A. **103**, 6160–6165
41 Beutler, E. (2008) Glucose-6-phosphate dehydrogenase deficiency: a historical perspective. Blood **111**, 16–24
42 Johnson, R. M., Goyette, Jr, G., Ravindranath, Y. and Ho, Y. S. (2000) Red cells from glutathione peroxidase-1-deficient mice have nearly normal defenses against exogenous peroxides. Blood **96**, 1985–1988
43 Lee, T. H., Kim, S. U., Yu, S. L., Kim, S. H., Park, D. S., Moon, H. B., Dho, S. H., Kwon, K. S., Kwon, H. J., Han, Y. H. et al. (2003) Peroxiredoxin II is essential for sustaining life span of erythrocytes in mice. Blood **101**, 5033–5038
44 Low, F. M., Hampton, M. B., Peskin, A. V. and Winterbourn, C. C. (2007) Peroxiredoxin 2 functions as a noncatalytic scavenger of low-level hydrogen peroxide in the erythrocyte. Blood **109**, 2611–2617
45 Arnér, E. S. and Holmgren, A. (2000) Physiological functions of thioredoxin and thioredoxin reductase. Eur. J. Biochem. **267**, 6102–6109
46 Siems, W. G., Sommerburg, O. and Grune, T. (2000) Erythrocyte free radical and energy metabolism. Clin. Nephrol. **53**, (Suppl), S9–S17

Received 30 January 2009/10 June 2009; accepted 10 June 2009
Published as BJ Immediate Publication 10 June 2009, doi:10.1042/BJ20090176

はじめに
Introduction

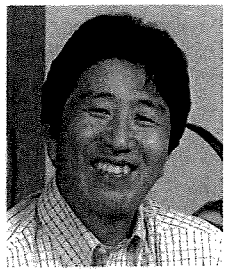

曽我朋義
Tomoyoshi SOGA
慶應義塾大学先端生命科学研究所

トランスクリプトミクス，プロテオミクス，メタボロミクス等のオミクス研究は細胞や生体内の多数の構成成分の変化をバイアスをかけない手法により網羅的に探索し，生命現象を包括的に理解しようとするものである．従来の仮説検証型の科学に対して，オミクスは網羅的なデータ解析によって背後に隠れている因子をみつけ出そうとする仮説発見型研究であり，だれも予想もしていなかった大発見をもたらす可能性を秘める．

今回はポストゲノム医学の新しい研究手法として最近注目を集めているメタボロミクスについて特集した．生物の活動は代謝とよばれるさまざまな酵素による化学反応の連鎖によって支えられている．代謝のおもな役割は外界から取り入れた物質をエネルギー(ATP)や，DNA，蛋白質などの生体高分子の前駆体(ヌクレオチド，アミノ酸など)あるいは脂質などに変換することである．代謝によって生産された代謝中間体や代謝産物の総称をメタボロームとよび，微生物で数百，哺乳動物で数千，植物で数万種類の代謝産物が存在するといわれている．

代謝物質は，物理的化学的性質が非常に似かよったものから，まったく異なるものまで数百種から数万種類存在するため，ひとつの分析法ですべてのメタボロームを測定することはいまだ困難である．しかし，ガスクロマトグラフィ-質量分析計(GC/MS)，高速液体クロマトグラフィ-質量分析計(LC-MS)，キャピラリー電気泳動-質量分析計(CE-MS)など定量的なメタボローム測定法が確立され，近年急速にメタボロミクスが医薬分野の基礎から応用研究に用いられるようになった．通常，代謝は高度に調節され，安定化されているが，代謝の異常で多くの疾患が引き起こされることや，癌細胞が異常な代謝を示すことなどは広く知られており，癌や疾病の機序解明や創薬開発には包括的に代謝を理解することが必要である．

本特集では，医薬分野で興味深いメタボローム解析を展開されている研究者に最新の成果を簡単に紹介していただいた．メタボロミクスはまだ生まれたばかりの方法論である．意欲的な人材がこの研究分野に参画し，新天地を切り開いてくれることを期待したい．

ヒト癌組織のメタボローム解析

Metabolome analysis of human tumor tissues

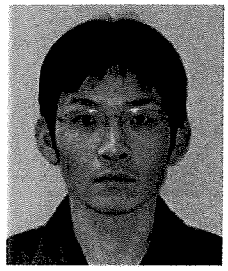

平山明由(写真)　曽我朋義
Akiyoshi HIRAYAMA and Tomoyoshi SOGA
慶應義塾大学先端生命科学研究所メタボローム解析グループ

◎キャピラリー電気泳動-質量分析装置(CE-MS)を用いたメタボローム測定法は，各種サンプル中に含まれるイオン性低分子代謝物の網羅的測定に適している．とくに解糖系，ペントースリン酸回路，TCA回路をはじめとして，アミノ酸代謝やプリン，ピリミジン代謝など，エネルギー代謝に関与する代謝物のほとんどはイオン性であることから，本法はエネルギー代謝を解明するうえで有用なツールになると考えられる．本稿ではCE-MSによるメタボローム解析を用いて，癌の微小環境における特殊なエネルギー代謝を明らかにした研究成果を紹介したい．

Key word：キャピラリー電気泳動-質量分析装置(CE-MS)，ワーバーグ効果，フマル酸呼吸

癌は周知のとおり，増殖，浸潤，転移を繰り返し，結果的にヒトを死に至らしめる疾患であるが，これまでに癌組織のエネルギー代謝を包括的に調べた研究例はほとんどない．通常，癌が増殖するためには膨大なエネルギー(ATP)が必要になるはずであるが，これら必要なエネルギーがどのように産生され，供給されているのかについては未知の部分も多い．メタボロームは生体内の代謝産物の総体を示す用語であるが，著者らはこれまでに，おもにキャピラリー電気泳動-質量分析装置(capillary electrophoresis-mass spectrometer：CE-MS)を用いたメタボローム解析を，微生物[1,2]，植物[3]，動物[4]などのサンプルに適用してきた．CE-MSは解糖系，ペントースリン酸回路，TCA回路をはじめとして，アミノ酸代謝，プリン代謝やピリミジン代謝などのエネルギー代謝に必須な代謝物群の一斉定量に有用な測定法である(「サイドメモ」参照)．

本稿では，CE-MSを用いたメタボローム解析を癌の微小環境における代謝の解明に応用し，得られた成果[5]を紹介する．

低酸素と癌のエネルギー代謝

癌細胞が好気的条件下においてもミトコンドリアでの呼吸を使わずに，おもに解糖系によってエネルギー産生を行う現象はワーバーグ効果[6]とよばれ，これまでにさまざまな癌種において確認されている．癌には，肝癌や胃癌のように比較的酸素分圧の高い癌と，膵癌や大腸癌のように癌細胞のまわりに血管がほとんどない(酸素分圧の低い)タイプの癌が存在し，一般的には後者のほうが増殖能力は高いといわれている．癌が増殖するには

サイドメモ　CE-MS

キャピラリー電気泳動(capillary electrophoresis：CE)と質量分析装置(mass spectrometer：MS)を並列につないだ分析装置の略称．内径数十μmのキャピラリー(毛細管)の中に泳動液を満たし，両端に数十kVの高電圧を印加することによって，キャピラリー内の物質をその電荷と水和イオン半径に基づいて分離した後，質量分析装置に導入することによって，高分離・高感度に検出する分析手法である．

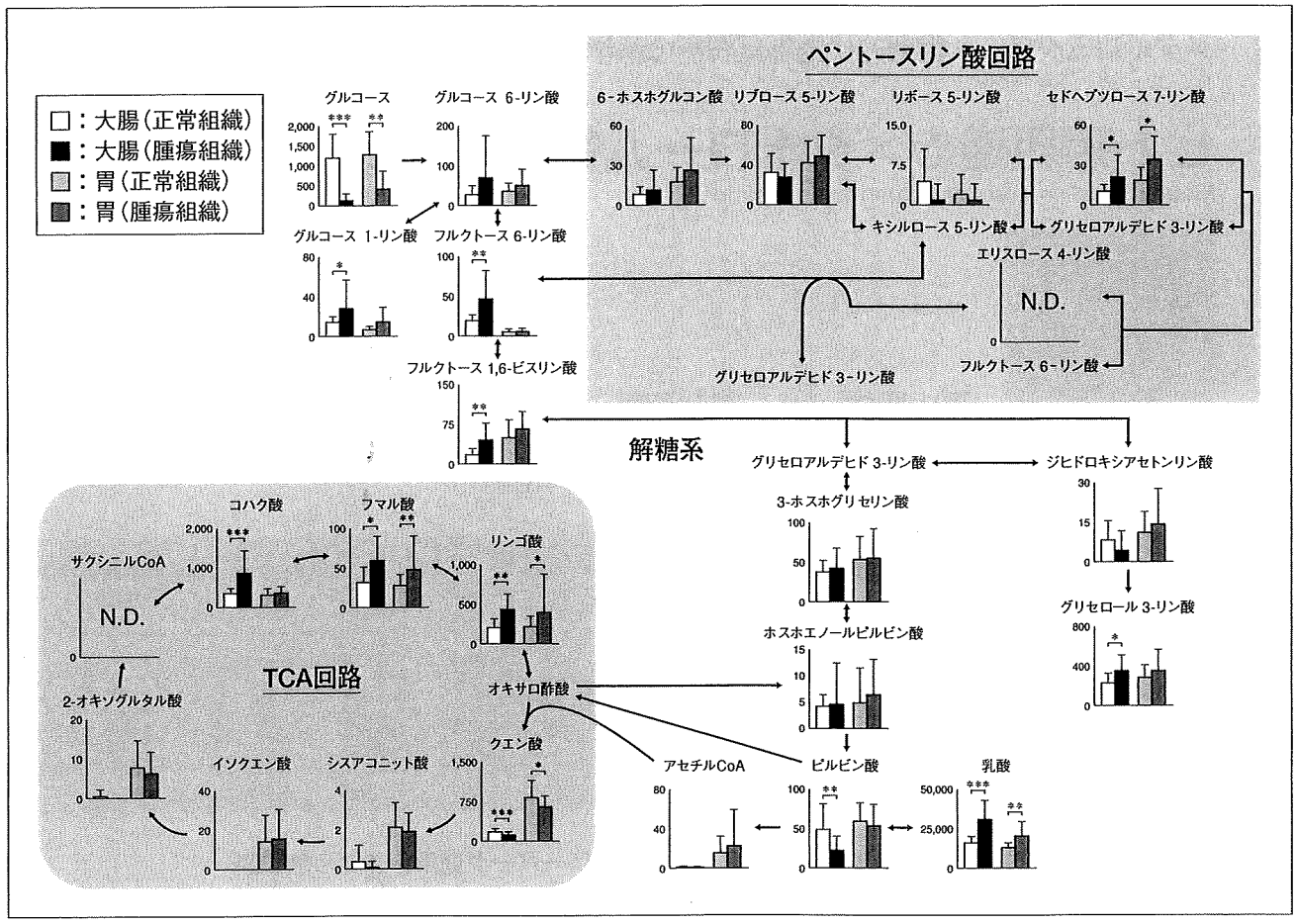

図 1　解糖系，ペントースリン酸回路，TCA回路に関与する代謝物の変動[5]

各代謝物量は 1 g 臓器当りの平均値±標準偏差で示してある．また，統計学的有意差の算出には Wilcoxon 検定を用いた．
*：$p<0.05$，**：$p<0.01$，***：$p<0.001$.

エネルギーとしての ATP が必要不可欠であるが，大部分の ATP は解糖系か酸化的リン酸化によって生産される．しかし，血管がないところで増殖する癌細胞は，解糖系に必要なグルコース量も酸化的リン酸化で必要な酸素も不足している．血流不足によって解糖系も酸化的リン酸化も制限された環境下においても増殖を続けられる癌細胞は，いったいそのエネルギーをどのように産生しているのであろうか．

そこで著者らは，キャピラリー電気泳動-飛行時間型質量分析装置(CE-TOFMS)を用いたメタボローム測定により，大腸癌および胃癌患者から採取した腫瘍組織および正常組織の代謝物質を一斉分析し，癌組織におけるエネルギー代謝のメカニズムの解明を試みた．

中心炭素代謝

今回，著者らは CE-TOFMS を用いたメタボローム測定によって，16 名の大腸癌患者，および 12 名の胃癌患者の腫瘍組織中から，約 800～1,100 種類の代謝物質由来と思われるピークを得た．そのうち，エネルギー代謝にとくに重要である解糖系，ペントースリン酸回路，TCA 回路の代謝中間体を代謝経路上にマッピングした結果を図 1 に示す．これらの代謝物に関しては標準物質を用いて各臓器 1 g 中の定量値を算出し，全サンプルの平均値をグラフに記載した．なお，グルコースに関しては液体クロマトグラフ-質量分析装置(LC-MS)を用いて定量値を算出した．

まず，腫瘍組織中のグルコース量はその正常組織中の量と比較して，大腸癌で約 1/10，胃癌では約 1/3 程度であった．さらに，これらは血中グルコース濃度と比較するとわずか 1/45(大腸癌)～1/13(胃癌)にしかならなかった(組織密度を 1 g/ml，血中グルコース濃度を 1 mg/ml と仮定した場合)．このことは生体内の癌が，最初に予想したと

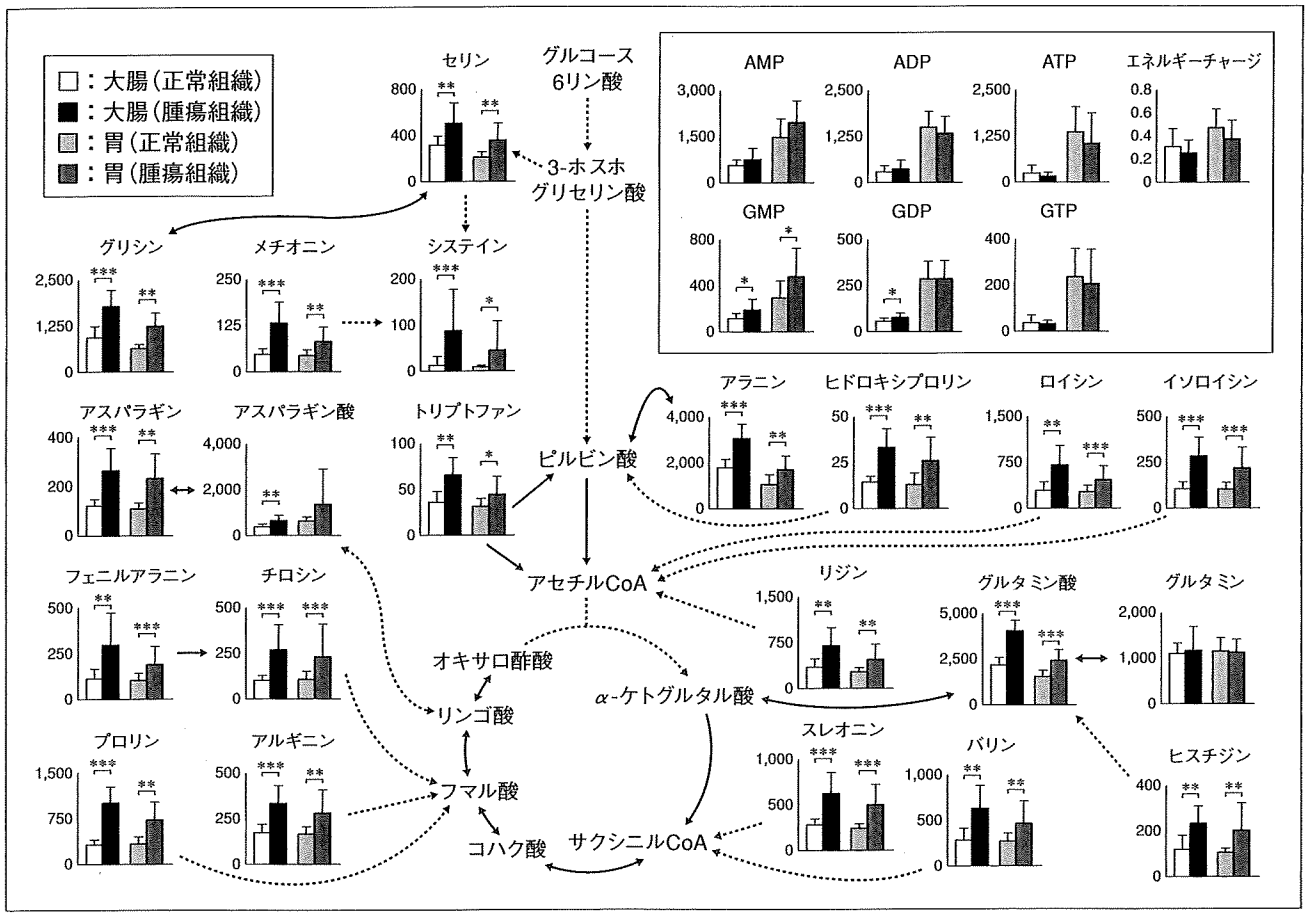

図 2　アミノ酸，ヒドロキシプロリン，ヌクレオチド類およびエネルギーチャージの変動[5]
各グラフの表示は図 1 と同じ．

おり血流の乏しい劣悪な環境下に存在していることを示唆している．一方で，解糖系の中間体物質量は非腫瘍組織と比べて同等かそれ以上であり，さらに解糖系の最終産物である乳酸量は両腫瘍組織において有意に高かった．このことから，Warburg が報告したように実際のヒトの腫瘍組織でも解糖系が亢進していることが明らかになった．

つぎに TCA 回路の代謝物に目を向けると，胃では正常，腫瘍組織とも TCA 回路の代謝中間体は一定量存在していたが，大腸では正常・腫瘍組織とも TCA 回路前半の代謝物(クエン酸からサクシニル CoA まで)がほとんど検出されておらず，ATP 量もきわめて低かった．大腸の酸素分圧は，胃のそれに比べて 1/5 程度という報告もあることから，おそらく大腸では正常組織も腫瘍組織も酸化的リン酸化反応はほとんど行われていないのではないかと推測される．

一方，TCA 回路後半の代謝物については癌特異的な傾向がみられた．とくに大腸の腫瘍組織において，TCA 回路の後半部分の代謝物(コハク酸，フマル酸，リンゴ酸)が有意に増加していた．この原因は謎であったが，寄生虫の呼吸にこの謎を解くヒントがあった．古くから嫌気性微生物や回虫などの寄生虫や二枚貝の一部では，嫌気的条件下でフマル酸呼吸とよばれる代謝によって ATP 産生が行われることが知られていた[7,8]．フマル酸呼吸は，電子伝達系における電子受容体として酸素の代りにフマル酸を用いて嫌気的に ATP を生成する反応であるが，その際に副生成物としてコハク酸を生じる．今回得られた大腸癌組織の結果においてもコハク酸が多く蓄積しており，嫌気的条件下での回虫の代謝パターンと類似していた．

一方，ある種の虫下し薬はフマル酸呼吸を阻害することが報告されており，著者らは虫下し薬を膵癌の培養細胞に添加すると癌細胞が死滅することをすでに実験で確かめている．これらを勘案した結果，現在のところ著者らは癌細胞もフマル酸呼吸かそれに類似した代謝によって ATP を産生

しているのではないかと考えている．

アミノ酸とヌクレオチド

図1に示したように，癌細胞では血流不足に伴い供給されるグルコース量も不足している．腫瘍組織はATP産生の一部をフマル酸呼吸に頼るとしても，それに必要なフマル酸はどこから供給されるのであろうか．図2に大腸および胃癌患者の正常，腫瘍組織のアミノ酸およびヌクレオチド量を示した．どちらの癌種においてもグルタミン以外のすべてのアミノ酸が有意に増加していた．血管新生が不十分な癌組織ではグルコース同様，血液からのアミノ酸の供給も不足していると考えられるため，これらのアミノ酸の増加は不思議である．

著者らは，必須アミノ酸も増加していること，ならびにコラーゲンの分解によって特異的に生成されることが知られているヒドロキシプロリン[9]量が増加していることから，腫瘍組織ではオートファージ[10,11]を活性化させることによりコラーゲンなどの周囲の蛋白質を積極的に分解し，ATPを生産するための前駆体としてアミノ酸を取り入れているのではないかと考えている．正常組織と腫瘍組織で唯一差のみられなかったグルタミンについては，グルタミノリシスという特殊な代謝がさまざまな癌種において活性化されている[12,13]ことがすでに知られている．つまり，癌細胞においてはグルタミンを特異的に消費する代謝経路が亢進しているために両組織間の差がなくなったものと考えられる．

最後に，大腸癌および胃癌の各組織におけるエネルギーチャージ[14]を比較した．興味深いことに，部分的にはまったく異なったエネルギー産生を行っているように思えたが，全体としてのエネルギーバランスは一定に保たれていることが証明された．

おわりに

本稿ではCE-MSを用いたメタボローム解析について，癌組織のエネルギー代謝の解明に応用した例をあげて紹介した．イオン性代謝物の一斉分析を可能にするCE-MSを用いて，著者らはすでに代謝調節メカニズムの解明，新規代謝経路の探索や各種バイオマーカーの探索など，基礎から応用に至るまでのさまざまなプロジェクトを推進し，成果を得つつある．本稿がCE-MSをはじめとしたメタボローム解析を理解していただく助けになれば幸いである．

謝辞：サンプル提供ならびにデータ解析に関してサポートをいただいた，国立がんセンター東病院の江角浩安病院長，小野塚博子博士，木下　平博士，斎藤典男博士，落合淳志博士，ならびに慶應義塾大学先端生命科学研究所の紙　健次郎氏，杉本昌弘博士，菅原真生氏，土岐尚子氏にこの場を借りて深謝致します．本研究は，厚生労働省癌研究助成金，文部科学省グローバルCOEプログラム“*In vivo* ヒト代謝システム生物学”，山形県および鶴岡市の支援によるものである．

文献

1) Ishii, N. et al.：Multiple high-throughput analyses monitor the response of E. coli to perturbations. *Science*, **316**：593-597, 2007.
2) Soga, T. et al.：Quantitative metabolome analysis using capillary electrophoresis mass spectrometry. *J. Proteome Res.*, **2**：488-494, 2003.
3) Sato, S. et al.：Simultaneous determination of the main metabolites in rice leaves using capillary electrophoresis mass spectrometry and capillary electrophoresis diode array detection. *Plant. J.*, **40**：151-163, 2004.
4) Soga, T. et al.：Differential metabolomics reveals ophthalmic acid as an oxidative stress biomarker indicating hepatic glutathione consumption. *J. Biol. Chem.*, **281**：16768-16776, 2006.
5) Hirayama, A. et al.：Quantitative metabolome profiling of colon and stomach cancer microenvironment by capillary electrophoresis time-of-flight mass spectrometry. *Cancer Res.*, **69**：4918-4925, 2009.
6) Warburg, O.：On the origin of cancer cells. *Science*, **123**：309-314, 1956.
7) Kita, K. et al.：Role of complex II in anaerobic respiration of the parasite mitochondria from Ascaris suum and *Plasmodium falciparum*. *Biochim. Biophys. Acta*, **1553**：123-139, 2002.
8) Ullmann, R. et al.：Transport of C(4)-dicarboxylates in Wolinella succinogenes. *J. Bacteriol.*, **182**：5757-5764, 2000.
9) Phang, J. M. et al.：The metabolism of proline, a stress substrate, modulates carcinogenic pathways. *Amino Acids*, **35**：681-690, 2008.
10) Droge, W.：Autophagy and aging-importance of amino acid levels. *Mech. Ageing Dev.*, **125**：161-168, 2004.
11) Mizushima, N. and Klionsky, D. J.：Protein turn-

over via autophagy : implications for metabolism. *Ann. Rev. Nutr.*, **27** : 19–40, 2007.
12) Medina, M. A. et al. : Relevance of glutamine metabolism to tumor cell growth. *Mol. Cell. Biochem.*, **113** : 1–15, 1992.
13) Moreadith, R. W. and Lehninger, A. L. : The pathways of glutamate and glutamine oxidation by tumor cell mitochondria. Role of mitochondrial NAD (P) + -dependent malic enzyme. *J. Biol. Chem.*, **259** : 6215–6221, 1984.
14) Chapman, A. G. et al. : Adenylate energy charge in *Escherichia coli* during growth and starvation. *J. Bacteriol.*, **108** : 1072–1086, 1971.

*　　*　　*

How to 発明 PART 2
全国発明表彰受賞者に聞く

平成21年度 発明協会会長賞

細胞内に存在する数千種類の低分子代謝物の一斉分析が初めて可能に

「メタボローム測定装置」の発明（特許第3341765号）

慶應義塾大学
環境情報学部 先端生命科学研究所 教授
曽我 朋義

1．今回の発明に至った経緯

生命科学では、これまでは謎であった生体や細胞の働きをつまびらかにすることによって、生命を理解し、その成果として人類が直面している健康、食糧、環境、エネルギーなどの問題の解決を目指しています。

生体を構成している細胞は、外界からグルコースなどの栄養源を取り入れ、それを代謝によって他の物質に変換し、活動に必要なエネルギー（ATP）や、アミノ酸、ヌクレオチド、脂質などの低分子化合物（代謝物）を生産しています。細胞には、代謝物が数百から数千種類存在しており、代謝物の総体をメタボロームと呼びます。

細胞の働きはゲノム情報に基づいており、メタボロームはゲノム情報の最終産物です。したがって、細胞の働きを担うゲノム、遺伝子、タンパク質等が変動すれば、最終産物である代謝物にも必然的に変化が生じるため、メタボローム解析によって細胞の状態や振る舞いを把握することができるのです。

近年、急速に発達したメタボローム研究は、代謝調節機構、遺伝子、タンパク質の機能解明といった生命科学の基礎研究に新しい解決策を提供しています。また最近では、疾患の機序解明、バイオマーカーの探索といった医薬分野、機能性成分の探索、ストレスに強い農作物の開発といった食品、農業分野、工業用微生物、バイオ燃料の開発といった工業、環境、エネルギー分野の応用研究にメタボローム研究が幅広く用いられるようになっています。

しかし、私がメタボローム解析に着手した2001年には、メタボローム測定の有用な方法論は存在していませんでした。

細胞には、物理的・化学的性質が非常に似通ったものから全く異なる代謝物が数百から数千種類存在しているため、これらを区別して測定することが極めて困難だったからです。

慶應義塾大学先端生命科学研究所*（山形県鶴岡市）のメタボロームプロジェクトに着任した私は、真っ先にメタボローム測定法の開発に取り組みました。

2．技術の概要

測定法を開発するに先立って、細胞内の代謝物の構造を調べると、ほとんどがイオン性の物質でした。最大数万種類の代謝物を一度に測定するには、イオン性物質に対して高分離能を持つキャピラリー電気泳動（CE）と高感度、高選択検出器である質量分析計（MS）を組み合わせたCE-MS法（図１）しかないと直感しました。

実際には、細胞から抽出した代謝物質を、内径が50μm、長さが１mの中空のキャピラリー（毛細管）の一端に注入し、３万Vの電圧をキャピラリーの両端に加えました。図２に示すように、陽イオン性代謝物質は陰極方向に泳動するため、陰極にMSを接続すれば、陽イオン性物質をすべてMSに導入することができます。MSを使い、その代謝物が固有に持つ質量でモニターすることにより、陽イオン性物質を一斉に測定することが可能になりました。反対に、陰イオン性代謝物は陽極方向に泳動するため、陽極にMSを接続することによって陰イオン性代謝物の

一斉分析が可能になりました。

3．技術的課題をどのように克服したか

しかし、CE-MSによるメタボローム測定法の開発は簡単ではありませんでした。当時、CE-MS法では、陰イオンの測定はできないというのが世界の常識でした。

CE-MSで陰イオンを測定すると、数分で電流値が流れなくなりました。最初は、なぜ電流が落ちるのか原因が分かりませんでした。試行錯誤した結果、図３に示すように、陽極側にMSを接続した場合に限り、電流が落ちることに気づきました。

CEで通常使用するフューズドシリカキャピラリーでは、電圧を印加すると、電気浸透流と呼ばれる液流が陽極から陰極方向に発生します（図３－①）。この影響で、数分たつと、キャピラリーの出口（MS側）に空気が入って絶縁されていることが判明しました（図３－②）。

電流が落ちる原因が電気浸透流が陰極方向に発生することだと分かったので、電気浸透流を陽極方向に反転させようと考えました。フューズドシリカキャピラリーの表面にあるシラノールは通常の条件では、H^+が解離して負に帯電します（図３－①）。電圧を印加すると、解離したH^+が陰極に一斉に移動することにより電気浸透流が陰極方向に発生します（図ではH^+は省略）。

電気浸透流を陽極方向に反転させるためには、キャピラリーからOH^-などの陰イオンを解離させる必要があります。そこで、キャピラリーに陽イオン性ポリマーをコーティングしたキャピラリーを試しました。

陽イオン性ポリマーがコーティングキャピラリーでは、OH^-が解離し（キャピラリー表面は正に帯電）、電圧を印加すると、OH^-は一斉に陽極に移動するため電気浸透流が陽極方向に発生するはずです（図３－③、OH^-は省略）。

予想どおり、このキャピラリーを使用することによって、電流が落ちることなく安定した陰イオン性物質の測定が可能になりました。本法が今回、受賞の対象となった発明です。

CE-MSによる陽イオンおよび陰イオンの分析法が完成し、イオン性物質の網羅的な測定が可能になりました。この方法を用いることによって、細胞内に存在する数千種類のイオン性代謝物の一斉分析が可能になり、メタボローム研究は飛躍的に発展しました。私たちは、現在40台のCE-MS装置を保有し（図４）、多くの研究成果が生まれています。

図１　CE-MS装置

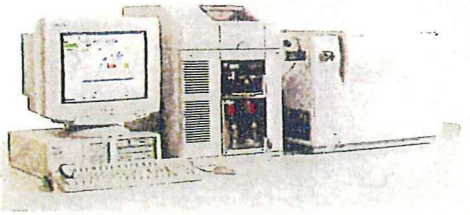

図２　CE-MSの分離の原理

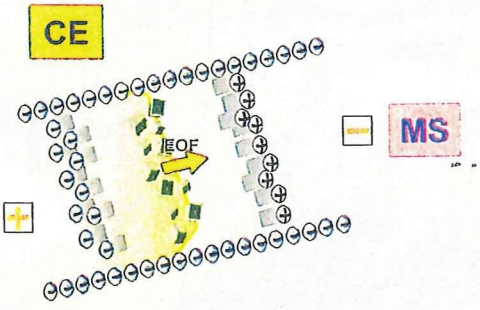

図３　CE-MSによる陰イオン性物質の測定法

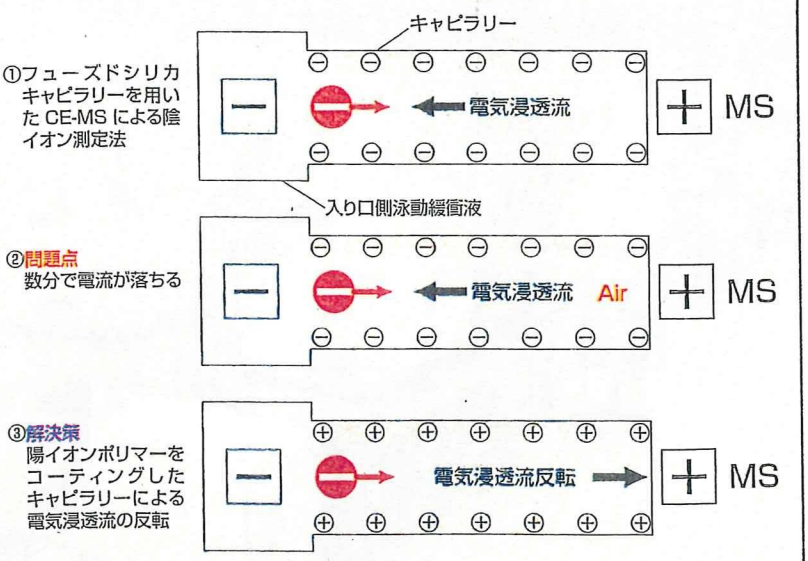

この発明のポイントは2つありました。CE-MSによる陰イオンの測定で電流が流れなくなる原因の究明と、安定した電気浸透流の反転法です。

電流が落ちることなく安定した陰イオンの測定を行うには、陽イオン性物質でコーティングされたキャピラリーを使うしかないという結論に達しましたが、そのような特殊なキャピラリーは市販されていませんでした。

ところが、当時、エーザイにいた石濱泰博士（現・慶應義塾大学先端生命科学研究所准教授）が、こんな物を作ったと私に送ってくれました。それは、まさに私が欲していた陽イオン性のポリマーでコーティングされたキャピラリーでした。

4. 研究・開発の“やりがい”と“心がけ”

いつも思っていることは、研究開発で行う実験が運良く成功しても、得るものは満足感以外何もないということです。実験が成功すると、人は考えることをあまりしません。

しかし、うまくいかないと何が問題だったかを真剣に考えます。仮説が間違っていたのか、実験条件や手順が悪かったのか等々。もし失敗の原因を究明し、解決できれば、それは自分だけの財産となります。

私の経験を振り返ると、自然界は偉大なもので、その実験結果はそうなるべくしてなっています。そのため、実験が思いどおりにならないということは、最初に立てた仮説が間違っている場合がほとんどです。自然界の法則に比べれば、自分の考えはなんて浅薄なのだろうと思い知らされることの連続でした。

これまで多くの研究を行ってきて、実験結果がなぜこうなるのか、分からないことがたくさんありました。しかし、その結果に関して何日も何日もあれこれ悩み考えている時間は結構楽しいものです。また、不思議なもので、朝から晩まで真剣に考えていると、入浴しているときや夢を見ているときに、その答えが思いつくことがあります。

うまくいかない原因が分かり、その問題が解決できたときの爽快感や達成感は、何物にも代えがたいものであり、研究者冥利に尽きます。

図4　慶應義塾大学先端生命科学研究所に並ぶ40台のCE-MSメタボローム測定装置

Cystathionine β-Synthase as a Carbon Monoxide–Sensitive Regulator of Bile Excretion

Tsunehiro Shintani,* Takuya Iwabuchi,* Tomoyoshi Soga, Yuichiro Kato, Takehiro Yamamoto, Naoharu Takano, Takako Hishiki, Yuki Ueno, Satsuki Ikeda, Tadayuki Sakuragawa, Kazuo Ishikawa, Nobuhito Goda, Yuko Kitagawa, Mayumi Kajimura, Kenji Matsumoto, and Makoto Suematsu

Carbon monoxide (CO) is a stress-inducible gas generated by heme oxygenase (HO) eliciting adaptive responses against toxicants; however, mechanisms for its reception remain unknown. Serendipitous observation in metabolome analysis in CO-overproducing livers suggested roles of cystathionine β-synthase (CBS) that rate-limits transsulfuration pathway and H_2S generation, for the gas-responsive receptor. Studies using recombinant CBS indicated that CO binds to the prosthetic heme, stabilizing 6-coordinated CO-Fe(II)-histidine complex to block the activity, whereas nitric oxide (NO) forms 5-coordinated structure without inhibiting it. The CO-overproducing livers down-regulated H_2S to stimulate HCO_3^--dependent choleresis: these responses were attenuated by blocking HO or by donating H_2S. Livers of heterozygous CBS knockout mice neither down-regulated H_2S nor exhibited the choleresis while overproducing CO. In the mouse model of estradiol-induced cholestasis, CO overproduction by inducing HO-1 significantly improved the bile output through stimulating HCO_3^- excretion; such a choleretic response did not occur in the knockout mice. *Conclusion:* Results collected from metabolome analyses suggested that CBS serves as a CO-sensitive modulator of H_2S to support biliary excretion, shedding light on a putative role of the enzyme for stress-elicited adaptive response against bile-dependent detoxification processes. (HEPATOLOGY 2009;49:141-150.)

Carbon monoxide (CO) is generated from inducible heme oxygenase 1 (HO-1) and constitutive heme oxygenase 2 (HO-2), respectively, and has the ability to regulate neurovascular functions,[1,2] apoptotic responses,[3,4] and metabolism of xenobiotics and toxicants.[5,6] This gas is overproduced through increased delivery of heme as a substrate and the HO-1 induction on exposure to stressors such as hypoxia and oxidative stress. Mechanisms by which CO regulates cell functions appear to involve an activation of soluble guanylate cyclase (sGC), the enzyme that allows the gas to bind to the prosthetic heme to synthesize cyclic guanosine monophosphate as a second messenger.[1] Distinct from nitric oxide (NO) that forms 5-coordinated NO-Fe(II) complex to trigger full activation of the enzyme, CO activates this enzyme only modestly because the gas binding stabilizes 6-coordinated CO-Fe(II)-histidine complex.[7] Mitogen-activated protein kinase has also been shown to serve as a CO-responsive signal transducer.[8] Gene disruption of HO-1 increases sensitivity to overproduction of reactive oxygen species, inflammatory mediators or xenobiotic metabolism, whereas the gene transfer or CO inhalation under these circumstances suppresses such pathogenic responses.[7-9] However, direct mechanisms for the CO reception to trigger these adaptive responses of metabolism remain unknown.

Because this gas has the ability to inhibit ferrous form of the prosthetic heme of enzymes, tryptophan 2,3-dioxygenase or cytochromes P450 have been considered puta-

Abbreviations: CBS, cystathionine β-synthase; CE-MS, capillary electrophoresis equipped with mass spectrometry; CO, carbon monoxide; CORM, CO-releasing metal carbonyl tricarbonyldichlororuthenium (II); ES, 17α-ethinylestradiol; GSH, glutathione; GSNO, S-nitrosyl glutathione; H12, liver exposed to 12-hour hemin treatment; NO, nitric oxide; $RuCl_3$, CO-free ruthenium (III) chloride; SAM, S-adenosyl methionine; SE, standard error; sGC, soluble guanylate cyclase.

From the Department of Biochemistry and Integrative Medical Biology, Department of Surgery, School of Medicine, Keio University, Tokyo, Japan; the Institute for Advanced Biosciences, Keio University, Tsuruoka City, Japan; and the First Department of Surgery, College of Medicine, Nagoya University, Nagoya, Japan.

Received July 3, 2008; accepted August 25, 2008.

**These authors contributed equally to this work.*

T.H. is a postdoctoral research fellow supported by Grant-in-Aid for Creative Scientific Research 17GS0419 from JSPS in Japan. Development of the methodology for differential metabolomic analyses using contrast-enhanced time of flight/mass spectrometry was supported by Leading Project for Biosimulation from MEXT. T.I. and T.Y. are research associates of Global COE Program for Metabolomic Systems Biology from MEXT and MHLW.

Address reprint requests to: Makoto Suematsu, M.D., Ph.D., Professor and Chair, Department of Biochemistry and Integrative Medical Biology, School of Medicine, Keio University, 35 Shinanomachi, Shinjuku-ku, Tokyo 160-8582, Japan. E-mail: msuem@sc.itc.keio.ac.jp; fax: (81)-3-5363-3466.

Published online in Wiley InterScience (www.interscience.wiley.com).

DOI 10.1002/hep.22604

Potential conflict of interest: Nothing to report.

tive CO-sensitive signal transducers regulating cell functions, including cell proliferation,[10] immune responses,[11] microvascular tone, xenobiotic detoxification, and biliary excretion in the liver.[5,6,12] However, ferrous heme of these enzymes is not only sensitive to CO but to NO. In this context, whether mechanisms by which CO regulates cell and organ functions is not shared by those for NO has not fully been studied yet.

This study aimed to mine novel CO-responsive regulators for stress-inducible adaptation of metabolism. To this end, we have used metabolome analyses based on capillary electrophoresis equipped with mass spectrometry (CE-MS) for systematic mining CO-responsive gaseous signal transducers. The current results suggest that cystathionine β-synthase (CBS), the enzyme rate-limiting transsulfuration pathway is such a novel CO-sensitive regulator of metabolism that plays an important role for quality control of bile excretion under disease conditions.

Materials and Methods

Preparation of Mice. The experimental protocols herein described were approved by our institutional guidelines provided by the Animal Care Committee of Keio University School of Medicine. Mice heterozygous for disruption in the CBS gene were purchased from Jackson Labs (Bar Harbor, MI) and bred at our institution. Male heterozygous CBS-deficient mice ($CBS^{+/-}$) and their littermates ($CBS^{+/+}$), and wild-type B6J mice, which were purchased from Clea Japan, Inc (Kawasaki City, Japan), were used at 8 to 12 weeks of age. Mice were allowed free access to laboratory chow and tap water, and were fasted for 18 hours before experiments. Mice were anesthetized with an intraperitoneal injection of ketamine at 120 mg/kg, and xylidine at 6 mg/kg. Their common bile ducts were ligated in proximity to the duodenum, and the gallbladder was nicked and cannulated with a polyethylene P-10 tube to collect bile for 20 minutes after a 10-minute stabilization period.[6,13] Biliary constituents such as total bile salts, bilirubin-IXα, pH values, and bicarbonate (HCO_3^-) were measured according to previous methods described elsewhere.[13] When necessary, biliary samples were collected into tubes containing 10% trichloroacetate to measure glutathione through high-performance liquid chromatography.[14] Determination of bilirubin-IXα in bile serves as an indicator of HO-mediated heme degradation in the liver that occurs in parallel with endogenous CO generation. Hepatic CO contents were also measured by gas chromatography as described previously,[15] except that the flame ionization detector equipped with a methanizer was used in this study instead of a reduction gas detector. Combination of these methods to determine CO allowed us to distinguish endogenous CO generation from the same gas exogenously administered as an intervention as described in the following session.

Administration of Reagents Studied. Protoheme IX (hemin) was administered at 40 μmol/kg intraperitoneally at 12 hours before surgical preparation for bile collection. This protocol was denoted as liver exposed to 12-hour hemin treatment (H12) treatment in the text. After collecting bile, livers were excised immediately to be snap-frozen in cold methanol, and the lysates served as samples for contrast-enhanced time of flight/mass spectrometry analyses as described later. In separate sets of experiments, liver samples were minced with 10% trichloroacetic acid at 4°C to measure cysteine and glutathione (GSH) through high-performance liquid chromatography to confirm the data collected from contrast-enhanced time of flight/mass spectrometry, when necessary.

A series of protocols were employed to examine roles of HO-derived CO in regulation of H_2S-modulated choleresis in the H12-treated mice. First, zinc protoporphyrin, a potent HO inhibitor, was administered intravenously at 12.5 μmol/hour/kg at 30 minutes before the bile collection; this dose was sufficient to block endogenous CO in the liver. When necessary, tricarbonyldichlororuthenium (II) dimer, the CO-releasing metal carbonyl [tricarbonyldichlororuthenium (II): CORM, Sigma-Aldorich][16] was administered intraportally at 30 minutes before the start of bile collection. When necessary, CO-free ruthenium (III) chloride ($RuCl_3$) was used as a negative control reagent. To examine whether the elevation of H_2S in the liver could alter biliary HCO_3^- excretion, sodium hydrosulfide (NaHS) was administered at 20 μmol/hour/kg through the portal vein at 30 minutes before the bile collection; as seen later in Results, this protocol restored the H12-induced decrease in the hepatic H_2S contents without altering a reduction of systemic blood pressure that was induced by a systemic bolus of the NaHS injection. S-nitrosyl glutathione (GSNO) was used as an NO donor. The reagent was injected intraportally with a dose of 7 μmol/kg at 30 minutes before the collection of bile; this protocol did not induce a reduction of systemic blood pressure, whereas greater doses caused hypotension and subsequent decrease in the bile output. In these experiments, administration of the reagent was performed through a 30-gauge miniature needle that was inserted into the portal vein to be fixed at the site of puncture. Finally, to examine therapeutic effects of CO, we examined effects of H12 treatment or administration of CORM in the mice exposed to drug-induced cholestasis. To this end, cholestasis was induced by a subcutane-

ous injection of 17α-ethinylestradiol (ES) at 5 mg/kg daily for 5 consecutive days before the experiments.[17]

Metabolome Analysis. We performed metabolome analyses of tissue lysates collected from snap-frozen livers of mice using contrast-enhanced time of flight/mass spectrometry according to our previous methods.[18,19] Measurements of hepatic H_2S contents were based on gas chromatography described in our previous method.[14] Biliary flux of bilirubin-IXα (BR-IXα) in bile samples were determined by enzyme-linked immunosorbent assay using the anti–BR-IXα monoclonal antibody as described previously.[6,20] Because BR-IXα is an end product of the HO-mediated degradation of protoheme IX, its measurements in bile serves as an index of endogenous CO generation in the liver.[20] The conversion of ^{15}N-methionine to its downstream metabolites was determined by CE-MS to examine different rates of the metabolic flux through CBS in the liver. In these experiments, ^{15}N-methionine was intraperitoneally injected at 150 μmol/100 g body weight, and ^{15}N-homocysteine and ^{15}N-cystathionine were measured by CE-MS using the lysates of liver tissues at 30, 60, and 120 minutes after the methionine challenge. Data were expressed as percentages of the mass-labeled metabolites versus total amounts of metabolites in remethylation cycle [ΣRM: methionine + S-adenosyl methionine (SAM) + S-adenosyl homocysteine (SAH) + homocysteine]. In a separate set of experiments, effects of application of CO on contents of methionine and cystathionine in HepG2 cells were determined in culture. In these experiments, the cells were maintained in Roswell Park Memorial Institute 1640 medium (Invitrogen, Carlsbad, CA) containing 10% fetal bovine serum; the mixture was supplemented with 1× penicillin/streptomycin and maintained at 37°C in an atmosphere of 5% CO_2/95% air. The cells were treated with either 50 μmol/L CORM or $RuCl_3$ as a negative control for 16 hours. To measure the metabolites, a frozen pellet of the 1×10^6 cells was homogenized in 10% trichloroacetic acid with 10 mM diethylene triamine pentaacetic acid following brief centrifugation, and the supernatant was used as a sample.

Western Blot Analysis. Western blot analysis was carried out to examine an induction of heme oxygenase (HO)-1 using the polyclonal antibody SPA896 (Stressgen, Ann Arbor, MI). In these experiments, the blotting against α-tubulin was carried out using the polyclonal antibody (Cell Signaling, Danvers, MA) as an internal control.

Recombinant Full-Length Rat CBS. The complementary DNA of the full-length rat CBS was a gift from Professor Masao Ikeda-Saito in Tohoku University. Stopped-flow equipment was purchased from Unisoku, Inc. (Tokyo) and used to examine binding of CO or NO to the CBS protein according to previous methods.[21] Electron paramagnetic resonance spectrometry to determine 5-coordinated structure of the nitrosylheme complex of CBS was carried out according to previous methods.[21,22]

Statistical Analyses. The statistical significance of data among different experimental groups was determined by one-way analysis of variance and Fischer's multiple comparison test. $P < 0.05$ was considered significant.

Results

CO Overproduction Inhibits Transsulfuration and H_2S and Stimulates HCO_3^- Choleresis. Metabolome analyses based on CE-MS allowed us to pinpoint metabolic pathways responding to disease conditions. In mouse liver, we detected more than 1800 metabolites, and compared differences between the control and acetaminophen-treated livers.[18] This method was used to determine differences in metabolic responses between mouse livers and those overloaded with heme, the stressor inducing oxidative stress and subsequent CO overproduction through increasing the substrate and inducing HO-1 (Fig. 1A). The hepatic CO flux peaked at 6 hours, becoming threefold to fourfold greater during the 6 to 12 hours after challenging with hemin, as judged by BR-IXα, an end product of HO-mediated heme degradation (Fig. 1B).[13] Under these conditions, bile output was modestly but significantly increased at 12 to 18 hours after the treatment (Fig. 1C) in parallel with significant elevation of HCO_3^- to make bile more alkaline (Fig. 1D-F), enhancing solubility of organic anions during the detoxification processes. These results suggest that the heme-elicited choleretic response is not correlated with vasodilatory mechanisms by the gas. Based on these results, we used CE-MS analyses to examine metabolomics in the liver exposed to 12-hour hemin treatment (H12), in which phenotypes of bile remodeling became evident.

Among known metabolites (Table 1), most prominent differences between the control and H12 groups occurred in global decreases in amino acids concurrent with increases in Krebs cycle substrates such as acetyl CoA: the fact that these changes coincided with sustained glutamate, significant increases in glutamine, and high-energy adenosine phosphates appeared to suggest utilization of the amino acid pool for energy substrates. By contrast, several essential amino acids such as methionine, tryptophan and histidine, and serine were maintained. Another important alteration was a global decrease in transsulfuration metabolites such as cystathionine, cysteine, and

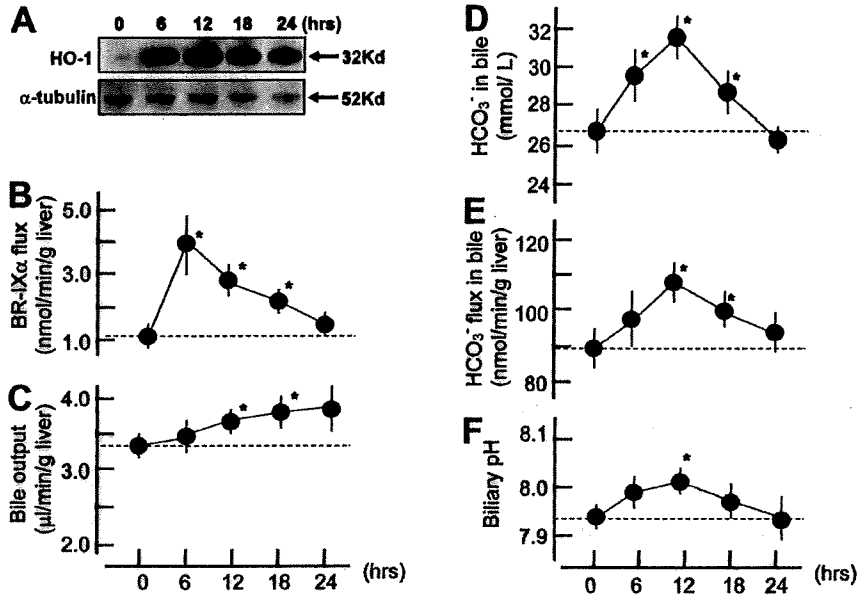

Fig. 1. Temporal alterations in hepatic generation of CO and biliary function after overloading heme. (A) Western blots indicating the induction of heme oxygenase (HO)-1. Alpha-tubulin is an internal control. (B) Biliary excretion of bilirubin-IXα (BR-IXα), a terminal metabolite of HO-dependent heme degradation, as an index of endogenous CO generation through heme oxygenase in the liver. (C) Bile output. (D) Biliary concentration of HCO_3^-. (E) Biliary flux of HCO_3^-. (F) pH values of bile. $^*P < 0.05$ versus the value measured at time 0, which is before the intraperitoneal hemin administration at 40 μmol/kg.

hypotaurine. These results led us to determine tissue contents of H_2S, the terminal product derived from CBS or cystathionine γ-lyase that constitute transsulfuration pathway; this gaseous compound turned out to be suppressed in the H12 group. Based on these measurements, we hypothesized that the H12 treatment limits the activity of CBS so far as judged from maintenance of methionine pool (ΣRM) and serine, a substrate of the enzyme, with suppression of the transsulfuration metabolites residing in the downstream (Fig. 2A). This hypothesis was confirmed by in vivo pulse-chase analysis showing accumulation of ^{15}N-homocysteine and suppression of ^{15}N-cystathionine after the ^{15}N-methionine challenge in the H12 group (Fig. 2B).

Such an inhibitory action of the H12 treatment on the transsulfuration pathway was reproducible when HepG2 cells was treated with CO in culture; contents of cystathionine were significantly suppressed by the application of 50 μmol/L CORM (9.3 ± 1.3 versus 15.9 ± 1.4 nmol/g protein for the vehicle treatment with $RuCl_3$. Mean ± standard error (SE) of three separate experiments, $P < 0.03$), whereas methionine exhibited no difference (66.3 ± 3.7 versus 80.3 ± 12.2 nmol/g protein for CORM and $RuCl_3$, respectively. Mean ± SE of three separate experiments), suggesting inhibitory action of the gas on CBS.

CO But Not NO Inhibits CBS. H12-induced metabolomic changes indicating dissociation between remethylation cycle and transsulfuration pathway led us to hypothesize that CBS, a heme-containing enzyme that rate-limits the transsulfuration pathway, is a sensor of the H12-elicited CO overproduction. Rat full-length recombinant CBS were purified (Fig. 3A) to examine whether CO or NO could inhibit the enzyme activities. CO, but not NO, specifically inhibited the enzyme (Fig. 3B). Previous crystallographic studies using a truncated form of CBS showed that the axial ligands for the prosthetic heme were cysteine and histidine, indicating a large peak of absorbance at 448 nm.[23] On CO application, the heme formed a 6-coordinated CO-Fe(II)–histidine complex, as judged by a decrease in the absorbance at 448 nm and a reciprocal elevation at 422 nm (Fig. 3C). These results were consistent with previous works using the truncated form of human recombinant CBS.[24] Such an inhibitory effect of CO on CBS activity occurred even when sufficient amounts of SAM were present as an allosteric activator,[25] whereas the CO concentrations necessary to suppress CBS became greater in the presence of SAM (Fig. 3D). Conversely, NO was able to bind to the heme but with a distinct structure of 5-coordinated nitrosyl-heme as judged by electron paramagnetic resonance spectrometry (Fig. 3E), suggesting that the enzyme responds specifically to the binding of CO but not that of NO.

CO-Induced HCO_3^- Choleresis Is Sensitive to H_2S and Disappears in $CBS^{+/-}$ Mice. Recent studies indicated that H_2S derived from cystathionine γ-lyase, an enzyme using cysteine to generate the gas, modulates biliary HCO_3^- excretion via mechanisms involving glibenclamide-sensitive channels, a putative H_2S target.[14,26] We hypothesized that the stress-induced CO stimulates the HCO_3^- excretion to increase pH in bile through its inhibitory action on CBS-derived H_2S. To examine this hypothesis, we chose the dose of the CO-releasing molecule (CORM) that was able to increase hepatic contents

Table 1. Comparison of Metabolome Analysis by CE-MS in Liver Extracts Between Control and the Hemin-Treated (H12) Mice

	Control	H12
Carbohydrates (nmol/g liver)		
Glucose 1-P	20 ± 4	31 ± 5
Glucose 6-P	24 ± 1	22 ± 6
Ribulose 5-P	206 ± 60	115 ± 17
Fructose 6-P	25 ± 1	21 ± 6
Glycerol 3-P	1800 ± 250	1663 ± 218
Lactate	3490 ± 633	2920 ± 385
Acetyl CoA	3.4 ± 0.5	6.2 ± 1.1*
Malonyl CoA	37 ± 6	83 ± 15*
Citrate	70 ± 13	88 ± 20
Fumarate	120 ± 22	167 ± 52
Malate	343 ± 91	479 ± 90
CoA	132 ± 21	111 ± 20
Nucleotides (nmol/g liver)		
ATP	208 ± 35	480 ± 90*
GTP	33 ± 4	79 ± 14*
ADP	577 ± 104	1060 ± 154*
AMP	1866 ± 277	1863 ± 70
IMP	501 ± 82	660 ± 99
Adenosine	203 ± 18	151 ± 11
Adenine	12 ± 1	12 ± 2
Hypoxanthine	58 ± 8	43 ± 15
	Control	**H12**
Amino acids (μmol/g liver)		
Gly	3.16 ± 0.11	2.20 ± 0.05*
Ala	3.12 ± 0.48	1.47 ± 0.40*
Ser	0.38 ± 0.07	0.31 ± 0.05
Pro	0.37 ± 0.03	0.27 ± 0.04*
Val	0.41 ± 0.01	0.23 ± 0.05*
Thr	0.31 ± 0.03	0.20 ± 0.04*
Lys	0.69 ± 0.13	0.46 ± 0.05*
Cys	0.20 ± 0.04	0.07 ± 0.03*
Leu	0.36 ± 0.02	0.25 ± 0.05†
Asp	0.76 ± 0.13	0.59 ± 0.12†
Glu	2.90 ± 0.16	2.75 ± 0.28
Gln	3.39 ± 0.58	6.48 ± 0.54*
His	0.43 ± 0.05	0.48 ± 0.02
Amino acids and derivatives (nmol/g liver)		
Met	49 ± 5	39 ± 10
GABA	29 ± 2	25 ± 4
Ornithine	420 ± 95	226 ± 22*
Asn	77 ± 7	59 ± 3*
Ile	175 ± 12	94 ± 17*
Arg	8.8 ± 1.2	4.8 ± 0.6*
Citrulline	64 ± 10	35 ± 3*
Trp	34 ± 2	31 ± 3
Tyr	111 ± 15	52 ± 8*
Glu-2 aminobutyrate	6.3 ± 2.3	5.7 ± 1.2
Ophthalmate	67 ± 7	83 ± 6

Data indicate mean ± SE of six separate experiments.
Data of metabolites in remethylation cycle and transsulfuration pathway were indicated in Fig. 2A.
*$P < 0.05$ and †$P < 0.1$ versus controls.

of CO comparably to those measured in the H12 treatment: As seen (Fig. 4A), the intraportal administration of CORM at 20 μmol/kg significantly increased hepatic CO contents comparable to those induced by H12 treatment in the intact mice. This dose of CORM suppressed hepatic H_2S and stimulated biliary HCO_3^- flux. Stimulatory effects of CO administration on biliary HCO_3^- excretion in intact mice were not shared by NO, as judged by observation in the mice administered with GSNO, an NO donor (Fig. 4B): These results were consistent with observation that CBS is sensitive to CO but not to NO in vitro (Fig. 3).

As already seen, H12 treatment increased CO generation (biliary BR-IXα flux), decreased hepatic H_2S contents, and stimulated biliary HCO_3^- flux (Fig. 1). HO blockade by zinc protoporphyrin-IX cancelled these changes elicited by H12 treatment. On the other hand, an administration of NaHS, an H_2S donor, abolished the H12-induced suppression of hepatic H_2S contents, and significantly attenuated the stimulatory response of biliary HCO_3^- flux (Fig. 5A), suggesting that H12-inducible CO stimulates biliary HCO_3^- excretion through modulation of CBS-derived H_2S. As previously reported, homozygous CBS knockout mice died of severe hepatic steatosis, whereas heterozygous knockout ($CBS^{+/-}$) mice survive through compensation without apparent phenotypes.[27] In these mice, indeed, the baseline H_2S content in livers of $CBS^{+/-}$ mice was comparable to that of $CBS^{+/+}$ mice, presumably because of compensation of the gas generation through cystathionine γ-lyase. On H12 treatment, $CBS^{+/-}$ mice exhibited an increase in the hepatic CO generation comparably to $CBS^{+/+}$ mice, but neither decreased H_2S contents nor up-regulated biliary HCO_3^- flux (Fig. 5B), indicating phenotypes distinct from those in $CBS^{+/+}$ littermates.

CO Protects Against Drug-Induced Cholestasis Through Mechanisms Involving CBS. We further attempted to investigate whether the administration of CO could improve biliary dysfunction occurring in disease models. To examine this, the mice were treated with ES, a cholestatic reagent suppressing three major osmolites such as HCO_3^-, glutathione, and bile salts in bile.[17] H12 treatment or the administration of CORM significantly increased bile output concurrently with a recovery of HCO_3^- excretion into bile (Fig. 6A). The anti-cholestatic effects of H12 treatment through stimulation of HCO_3^- excretion disappeared in the $CBS^{+/-}$ mice (Fig. 6B), suggesting again a pivotal role of CBS for triggering the CO-induced choleresis.

Discussion

CO administration or HO-1 induction has been shown to protect against tissue injury and considered a potentially useful therapeutic stratagem.[8,16] Serendipitous observation in the liver indicating effects of overproduced CO on metabolism of sulfur-containing amino